

Title	Copper isotope fractionation between aqueous compounds relevant to low temperature geochemistry and biology
Author(s)	Fujii, Toshiyuki; Moynier, Frédéric; Abe, Minori; Nemoto, Keisuke; Albarède, Francis
Citation	Geochimica et Cosmochimica Acta (2013), 110: 29-44
Issue Date	2013-06
URL	http://hdl.handle.net/2433/173360
Right	© 2013 Elsevier Ltd.
Type	Journal Article
Textversion	author

1 Original Paper

2

3

4 **Copper isotope fractionation between aqueous compounds**

5 **relevant to low temperature geochemistry and biology**

6

7 Toshiyuki Fujii^{1*}, Frédéric Moynier², Minori Abe³,

8 Keisuke Nemoto³, and Francis Albarède⁴

9

10 ¹ Research Reactor Institute, Kyoto University, 2-1010 Asashiro Nishi, Kumatori,
11 Sennan, Osaka 590-0494, Japan

12 ² Department of Earth and Planetary Sciences and McDonnell Center for Space
13 Sciences, Washington University in St. Louis, Campus Box 1169, 1 Brookings Drive,
14 Saint Louis, MO 63130-4862, USA

15 ³ Department of Chemistry, Graduate School of Science and Engineering, Tokyo
16 Metropolitan University, 1-1 Minami-Osawa, Hachioji-shi, Tokyo 192-0397, Japan

17 ⁴ Ecole Normale Supérieure de Lyon, Université de Lyon 1, CNRS, 46, Allée d'Italie,
18 69364 Lyon Cedex 7, France

19

20

21 *Author to whom correspondence should be addressed

22 tosiyuki@rri.kyoto-u.ac.jp

23 TEL: +81-72-451-2469, FAX: +81-72-451-2634

24

25 **Abstract:**

26 Isotope fractionation between the common Cu species present in solution (Cu^+ , Cu^{2+} ,
27 hydroxide, chloride, sulfide, carbonate, oxalate, and ascorbate) has been investigated
28 using both *ab initio* methods and experimental solvent extraction techniques. In order to
29 establish unambiguously the existence of equilibrium isotope fractionation (as opposed
30 to kinetic isotope fractionation), we first performed laboratory-scale liquid-liquid
31 distribution experiments. Upon exchange between HCl medium and a macrocyclic
32 complex, the $^{65}\text{Cu}/^{63}\text{Cu}$ ratio fractionated by -1.06 to -0.39% . The acidity dependence
33 of the fractionation was appropriately explained by ligand exchange reactions between
34 hydrated H_2O and Cl^- via intramolecular vibrations. The magnitude of the Cu isotope
35 fractionation among important Cu ligands was also estimated by *ab initio* methods. The
36 magnitude of the nuclear field shift effect to the Cu isotope fractionation represents only
37 $\sim 3\%$ of the mass-dependent fractionation. The theoretical estimation was expanded to
38 chlorides, hydroxides, sulfides, sulfates, and carbonates under different conditions of
39 pH. Copper isotope fractionation of up to 2% is expected for different forms of Cu
40 present in seawater and for different sediments (carbonates, hydroxides, and sulfides).
41 We found that Cu in dissolved carbonates and sulfates is isotopically much heavier
42 ($+0.6\%$) than free Cu. Isotope fractionation of Cu in hydroxide is minimal. The
43 relevance of these new results to the understanding of metabolic processes was also
44 discussed. Copper is an essential element used by a large number of proteins for
45 electron transfer. Further theoretical estimates of $\delta^{65}\text{Cu}$ in hydrated Cu(I) and Cu(II)
46 ions, Cu(II) ascorbates, and Cu(II) oxalate predict Cu isotope fractionation during the
47 breakdown of ascorbate into oxalate and account for the isotopically heavy Cu found in
48 animal kidneys.

49

50 **Keywords:** Copper, Cupric, isotope fractionation, ligand, quantum chemical calculation

51

1. INTRODUCTION

Copper has two stable isotopes, ^{63}Cu and ^{65}Cu , with respective average abundances of 69.174% and 30.826% in the reference metal SRM-NIST 976 (Shields et al., 1964). Variations of Cu isotope abundances in natural samples were identified by Walker et al. (1958) using thermal ionization mass spectrometry, but the variability of the mass bias at that time was too large with respect to the natural isotopic availability to qualify Cu isotopes as a potential geochemical or biochemical tracer. The advent of inductively-coupled plasma mass spectrometry (ICP-MS) instruments equipped with a magnetic sector and multiple collection made precise isotopic analysis of Cu possible (Albarède, 2004). Maréchal et al. (1999) published the first measurements of Cu isotope compositions in a variety of minerals and biological materials. The broad range of isotopic variations in Cu ores observed previously (Walker et al. 1958; Shields et al., 1965) was confirmed by subsequent work (Maréchal et al., 1999; Zhu et al., 2000; Albarède, 2004; Klein et al., 2009). Hereafter, the δ notation with

$$\delta^{65}\text{Cu} = \left(\frac{([\text{}^{65}\text{Cu}]/[\text{}^{63}\text{Cu}])_{\text{sample}}}{([\text{}^{65}\text{Cu}]/[\text{}^{63}\text{Cu}])_{\text{reference}}} - 1 \right) \times 1000 \quad (1)$$

is used throughout.

The narrow range of Cu isotope variation in basalts (Ben Othman et al., 2006; Archer and Vance, 2004; Herzog et al., 2009; Li et al., 2009; Moynier et al., 2010; Bishop et al., 2012) and granites (Li et al., 2009) suggests that high-temperature magmatic processes do not induce large Cu isotope fractionation. As a consequence, it makes Cu isotopes a tracer of choice for the study of sediments and more generally for

73 low-temperature processes such as those involved in soil formation (Bigalke et al., 2010,
74 2011) and in biology (Balter and Zarro, 2011; Weinstein et al., 2011).

75 Substantial isotope fractionation during chemical exchange reactions occurs at
76 room temperature and reflects isotopic differences between the equilibrium constants of
77 Cu isotopologues. Enrichment in ^{65}Cu of up to 0.8‰ was observed during the
78 chromatographic elution of compounds (Matin et al., 1998; Maréchal et al., 1999, 2002;
79 Zhu et al., 2002). The same technique demonstrates isotope fractionation of ~0.4‰
80 upon chromatographic separation of Cu(I) from Cu(II) (Matin et al., 1998; Zhu et al.,
81 2002).

82 At low temperature, Cu isotopic abundances are also affected by inorganic
83 surface processes (physical adsorption/desorption). Isotope separation of up to a few
84 permil upon adsorption/desorption of Cu onto/from inorganic and organic substrates
85 was observed by several groups (Mathur et al., 2005; Balistrieri et al., 2008; Pokrovsky
86 et al., 2008; Navarette et al., 2011).

87 Copper plays very important roles in biology (Lippard and Berg, 1994). The
88 metal centers of the ‘blue’ copper proteins are divided according to the coordination of
89 the Cu ion into three types that contain one or more copper ions as prosthetic groups
90 (Cowan, 1997). In plastocyanine, cysteine, histidine, and methionine ‘residues’ bind to
91 Cu and this plays a major role for electron transfer (redox reactions) (Freeman and Guss,
92 2001). In humans, ceruloplasmin is a ferroxidase enzyme involved in the iron cycle,
93 cytochrome c oxidase is involved in electron transfer across the membrane of
94 mitochondrion, and superoxide dismutase protects cells against superoxide. Blue (Cu)
95 proteins are ubiquitous and characterized by their multiple ways of bonding with amino
96 acids. (Cowan, 1997). Coupling of Fe and Cu isotope fractionation has been identified

97 in human blood components (Albarède et al., 2011a) and in mammals (Balter and Zazzo,
98 2011; Albarede et al., 2011b). Depletion of $\delta^{65}\text{Cu}$ at the permil level was found in plants
99 with respect to soils or nutrient solutions (Weinstein et al., 2011; Jouvin et al., 2012).
100 $\delta^{65}\text{Cu}$ in enzymes is a few permil negative compared with the Cu isotopic composition
101 of the host soil (Zhu et al., 2002). Positive $\delta^{65}\text{Cu}$ values up to 1.5‰ also were found in
102 the kidneys of sheep (Balter and Zazzo, 2011) and mice (Albarede et al., 2011b).

103 Contrary to Fe (Hill et al., 2010; Rustad et al., 2010, and references therein), Ni
104 (Fujii et al., 2011a), and Zn (Fujii et al., 2010,2011b; Black et al., 2011; Pons et al.,
105 2011; Fujii and Albarède, 2012), the theoretical prediction of Cu isotope fractionation
106 among ligands (simple inorganic ligands like halide, sulfate, and phosphate ions, and
107 more complex organic ligands as humic acids and phytoplankton exometabolites) in
108 natural waters and biological fluids has only received minimal attention, which is a
109 major hindrance for an informed interpretation of observations. This is the main
110 motivation for the present work.

111 We first demonstrate that equilibrium isotope fractionation of Cu(II) does take
112 place in laboratory-scale experiments. In parallel, we calculated the molecular orbitals
113 of the corresponding Cu species to obtain the reduced partition function ratio (RPFR) of
114 isotopologues. The *ab initio* calculations were then extended to hydrated Cu(II)
115 complexes, hydroxide, sulfate, carbonate, ascorbate, and oxalate. The choice of
116 ascorbate and oxalate was motivated by evidence of isotopically heavy Cu in the
117 kidneys of sheep (Balter and Zazzo, 2011) and mice (Albarède et al., 2011b). Ascorbate
118 is allegedly catabolized into oxalic acid (Chai et al., 2004; Massey et al., 2005;
119 González et al., 2005), which makes some patients develop a condition known as
120 hyperoxaluria and develop kidney stones, a calcium oxalate. The oxalate anions are

121 known to be strong complexing ligands of Cu(II) (Hayakawa et al., 1973), while
122 ascorbate oxidase, which oxidizes ascorbate into dehydroascorbate (Solomon et al.,
123 1996) is a bis(histidine)copper(II) compound. Applications of our calculations to the
124 understanding of Cu isotope variability in marine sediments and to biological samples
125 are briefly outlined.

126

127

2. METHODS

128 2.1. Extraction experiments and isotopic analyses

129 Dicyclohexano-18-crown-6 (DC18C6) (>97% purity) is a product of Fluka
130 Chemie GmbH and Cu dichloride (hydrated, 99.9% purity) is a product of Wako Pure
131 Chemical Industries, Ltd. Hydrochloric acid, in which the Cu impurity was certified to
132 be less than 1.9 ppt, was purchased from Kanto Chemical, Co., Inc. Other chemicals
133 were reagent grade.

134 $\text{CuCl}_2 \cdot 2\text{H}_2\text{O}$ was dissolved in HCl to prepare solutions of 0.1 mol dm^{-3} (M)
135 Cu(II) in 1 to 6 M HCl. DC18C6 was dissolved in 1,2-dichloroethane to prepare a
136 solution of 0.1 M DC18C6. Ten mL aqueous solution were combined with 15 mL
137 organic solution in a glass vial, which was sealed. The two phases were stirred for 30
138 minutes using a Teflon-coated magnetic bar. After equilibrium was achieved, the two
139 phases were separated by centrifugation at 2,000 rpm for 1 min, and an aliquot of the
140 aqueous solution taken for analysis. A 10 mL aliquot of the organic solution was saved
141 for back extraction of Cu in 15 mL of 0.02 M HCl. The extracted Cu was fully (>98%)
142 recovered in this procedure. All these steps were carried out at 298 K. Copper
143 concentrations in the equilibrated aqueous phase and the back extraction solution were
144 determined by inductively-coupled plasma atomic-emission spectrometry (Thermo

145 Fisher Scientific, iCAP 6300 Duo). Aliquots of these solutions were saved for isotopic
146 analysis.

147 Organic impurities carried over from the extraction step were separated from
148 Cu on AGMP1 anion exchange resin in 7 M HCl as described in Maréchal et al. (1999).
149 Copper isotopic compositions were measured on a Thermo-Finnigan Neptune
150 MC-ICP-MS at Washington University in St. Louis. The samples were introduced by
151 free aspiration in 0.1 M HNO₃ using a Teflon microcentric nebulizer (uptake rate of 100
152 μL/min) and a glass cyclonic spray chamber. Masses 63 and 65 were positioned on the
153 L2 and axial collectors, respectively. Intensities of Zn isotopes (64, 66, 67 and 68) were
154 measured on the collectors L1, H1, H2, H3, respectively. The intensity of ⁶²Ni was
155 monitored in order to correct for the potential interference of ⁶⁴Ni. Instrumental mass
156 fractionation was corrected by both Zn doping and standard-sample bracketing
157 (Maréchal et al., 1999; Albarède, 2004). The typical external reproducibility of replicate
158 analyses of the same samples carried out during different analytical sessions is 0.10‰
159 (2σ) for δ⁶⁵Cu.

160

161 **2.2. Computational methods**

162 Orbital geometries and vibrational frequencies of aqueous Cu(II) species were
163 computed using the density functional theory (DFT) as implemented by the Gaussian09
164 code (Frisch et al., 2009; Dannington et al., 2009). The DFT method employed here is a
165 hybrid density functional consisting of Becke's three-parameter non-local hybrid
166 exchange potential (B3) (Becke, 1993) with Lee-Yang-and Parr (LYP) (Lee et al., 1988)
167 non-local functionals. Using the 6-311+G(d,p) basis set or higher is recommended for
168 calculating the Cu complexes by de Bruin et al. (1999). The 6-311+G(d,p) basis set,

169 which is an all-electron basis set, was therefore chosen for H, C, O, S, Cl, and Cu.
170 Molecules were modeled without any forced symmetry. An ‘ultrafine’ numerical
171 integration grid was used and the SCF (self-consistent field) convergence criterion was
172 set to 10^{-9} .

173 The isotope enrichment factor due to intramolecular vibrations can then be
174 evaluated from the reduced partition function ratio $(s/s')f$ (Bigeleisen and Mayer, 1947),
175 also noted β ,

$$\ln \frac{s}{s'} f = \sum [\ln b(u_i') - \ln b(u_i)] \quad (2)$$

176 where

$$\ln b(u_i) = -\ln u_i + \frac{u_i}{2} + \ln(1 - e^{-u_i}) \quad (3)$$

177 and

$$u_i = \frac{h\nu_i}{kT} \quad (4)$$

178

179 in which ν stands for vibrational frequency, s for the symmetry number of the Cu
180 compound, h the Planck constant, k the Boltzmann constant, and T the absolute
181 temperature. The subscript i denotes the i th mode of molecular vibration, and primed
182 variables refer to the light isotopologue. The isotope enrichment factor due to molecular
183 vibrations can be evaluated from the frequencies (ν) summed over all the different
184 modes. The isotopic difference in the stability constant of chemical reactions is identical
185 to the difference of $\ln \beta$ between related species. For example, a chemical exchange
186 reaction,



187

188 with stability constant K_{CuCl^+} , the isotope fractionation between the hydrated Cu^{2+} and

189 $CuCl^+$ is,

$$\ln \frac{K_{CuCl^+}({}^{65}Cu)}{K_{CuCl^+}({}^{63}Cu)} = \ln \frac{[{}^{65}CuCl^+]/[{}^{63}CuCl^+]}{[{}^{65}Cu^{2+}]/[{}^{63}Cu^{2+}]}$$

190

$$= \ln \beta_{CuCl^+} - \ln \beta_{Cu^{2+}} \quad (6)$$

191

192 Isotope fractionation also results from the mass-independent nuclear field shift
193 effect (Bigeleisen, 1996; Nomura et al., 1996, Fujii et al. 2009) which is an

194 isotope-dependent shift reflecting that the electronic orbitals do not vanish at the

195 nucleus and depends on the nuclear size and shape (King, 1984). The latest version of

196 quantum chemical models have taken finite-size nuclei into account in *ab initio*

197 calculations (Schauble, 2007; Abe et al., 2008, 2010; Fujii et al., 2010, 2011a,c,d). For

198 light elements such as Ni (Fujii et al., 2011a) and Zn (Fujii et al., 2010), the nuclear

199 field shift effect was found to be small as 0.02-0.03%/amu. The isotope enrichment

200 factor via the nuclear field shift ($\ln K_{fs}$) is given by

201

$$\ln K_{fs} = \frac{hc}{kT} \nu_{fs} \quad (7)$$

202

203 where ν_{fs} is the nuclear field shift and c the velocity of light.

204 The contribution of the nuclear volume was estimated by the Dirac-Coulomb

205 Hartree-Fock (DCHF) method implemented in the UTChem program (see references in

206 Abe et al., 2008, 2010). We calculated the electronic structure of $\text{Cu}^0([\text{Ar}]3d^{10}4s^1)$,
207 $\text{Cu}^+([\text{Ar}]3d^{10})$, $\text{Cu}^{2+}([\text{Ar}]3d^9)$ and a few other simple Cu molecules. The Cartesian
208 coordinates of Cu molecules optimized by the Gaussian09 code were supplied to the
209 DCHF calculation. Exponents of basis sets were taken from Faegri's four-component
210 basis for Cu (Faegri, 2001), third-order Douglas-Kroll basis for H and Cl (Tsuchiya et
211 al., 2001), and ANO-RCC for O (Roos et al., 2005). Contraction coefficients were
212 optimized by four-component atomic calculations (Koc and Ishikawa, 1994). After
213 adding some diffuse and polarization functions, the final contraction form of the large
214 component basis sets was $(19s14p9d)/[6s4p3d]$ for Cu, $(16s11p1d)/[4s3p1d]$ for Cl,
215 $(14s9p2d)/[3s2p2d]$ for O, and $(8s2p)/[3s2p]$ for H.

216 The effect of nuclear spin can be neglected at equilibrium (Bigeleisen, 1996).
217 Since the present crown ether experiments were run at equilibrium, the kinetic part of
218 this effect also known as the magnetic isotope effect (Epov et al., 2011; Epov, 2011),
219 will not be considered in this work.

220

221 3. RESULTS AND DISCUSSION

222 3.1. Isotope fractionation of Cu by crown ether extraction

223 The Cu(II) species in HCl medium in the laboratory experiment are Cu^{2+} ,
224 CuCl^+ , CuCl_2 , and CuCl_3^- (Brugger et al., 2001), which are related through
225 complexation reaction 5 and the following stepwise reactions, with stability constants
226 K_{species} ,



227 and



228

229 The presence of CuCl_4^{2-} was reported for highly concentrated HCl and CuCl_2 systems
 230 (Bell et al., 1973; Neilson, 1982; Tanimizu et al., 2007) or high-temperature systems
 231 (Collings et al., 2000) but this higher order of complexation is negligible at the low HCl
 232 concentrations and ambient temperature of the present experiments (Brugger et al.,
 233 2001).

234 The extraction reaction of Cu(II) with the macrocyclic ligand can be written as,



235

236 where L stands for DC18C6. The distribution ratio D is written as,

$$D = \frac{\Sigma[\text{Cu(II)}]_{\text{org}}}{\Sigma[\text{Cu(II)}]_{\text{aq}}} \approx \frac{[\text{CuLCl}_2]}{[\text{Cu}^{2+}] + [\text{CuCl}^+] + [\text{CuCl}_2] + [\text{CuCl}_3^-]} \quad (11)$$

237

238 where the subscripts 'org' and 'aq' stand for the organic and aqueous phases,
 239 respectively.

240 The isotope separation factor α , between the aqueous and organic phases, is
 241 defined as:

$$\alpha = \frac{\sum_k \phi_{\text{org}}^k \left(\frac{^{65}\text{Cu}}{^{63}\text{Cu}} \right)_{\text{org}}^k}{\sum_k \phi_{\text{aq}}^k \left(\frac{^{65}\text{Cu}}{^{63}\text{Cu}} \right)_{\text{aq}}^k} \quad (12)$$

242

243 where k refers to the k th compound in the organic and aqueous phases, respectively, and
244 φ is the fraction of total Cu (proper ^{63}Cu) hosted in the k th compound. The isotope
245 enrichment factor is defined as $\alpha - 1$. Because α is always close to unity, $\alpha - 1 \approx \ln \alpha$,
246 and $1000 \ln \alpha$ therefore can be approximated by $\Delta^{65}\text{Cu} = \delta^{65}\text{Cu}_{\text{org}} - \delta^{65}\text{Cu}_{\text{aq}}$. The $\Delta^{65}\text{Cu}$
247 values obtained are shown in Table 1 together with distribution ratios. $\Delta^{65}\text{Cu}$ ranged
248 from -1.06 to -0.39% .

249 The yield of Cu(II) extraction by crown ethers has been investigated by Yoshio
250 et al. (1980), Nakamura et al. (1982), and Contreras et al. (1993). A study on extraction
251 kinetics showed that equilibrium is achieved within 30 sec (Nakamura et al., 1982).
252 Hydration-dehydration is known to be the rate-limiting step of solvent extraction. The
253 rate constant for H_2O substitution in the inner coordination sphere of Cu^{2+} is quite high
254 in the transition metal series, and it is comparable with that of Li^+ of the alkali metals as
255 observed by Eigen (1963). The isotope exchange rate kinetics of $^7\text{Li}/^6\text{Li}$ in the crown
256 ether systems has been studied in detail (Jepson and Cairns, 1979; Nishizawa et al.,
257 1984), in which the isotopic equilibrium is achieved within 30-60 sec after contacting
258 aqueous and organic phases. The 30 min stirring period in the present study is therefore
259 considered to be enough to achieve the isotopic equilibrium of Cu. The $\Delta^{65}\text{Cu}$ values
260 listed in Table 1 are hence attributable to the equilibrium isotope effect.

261 Figure 1a shows the mole fractions of Cu species estimated by using the
262 stability constants of reactions 5, 8, and 9 (Brugger et al., 2001). $\Delta^{65}\text{Cu}$ was found to
263 vary with HCl molarity (Fig. 1b), a trend that reflects the isotope fractionation of Cu in
264 reactions 5 and 8-10. With increasing HCl molarity, more CuCl_2 forms, which in turn
265 results in an increase of D . The magnitude of $\Delta^{65}\text{Cu}$ shown in Table 1 is similar to that

266 found in other ligand exchange systems (Matin et al., 1998; Maréchal et al., 1999, 2002;
267 Zhu et al., 2002).

268

269 **3.2. Contribution of the mass-independent isotope effect**

270 The total electronic energies calculated for Cu isotopes and isotopologues are
271 shown in atomic units (a.u.) in Table 2, in which Cu^{2+} was chosen as the reference. The
272 maximum effect was found to be 0.015‰ for the Cu^0 -Cu(I) pair and 0.012‰ for the
273 Cu(I)-Cu(II) pair. The solvent extraction reaction is controlled by ligand exchange of
274 Cu(II). Based on the Cu(II) data in Table 2, the nuclear field shift effect in Cu(II)
275 species is only ~3% of the smallest $\Delta^{65}\text{Cu}$ value listed in Table 1. The values of $\Delta^{65}\text{Cu}$
276 reported in Table 1 are the values for the mass-dependent isotope fractionation and
277 reflect intramolecular vibrations.

278

279 **3.3. Mass-dependent isotope effects**

280 *3.3.1. Hydrated Cu(II) ions*

281 The hydrated Cu(II) ion is generally represented as the hexaaqua complex
282 $\text{Cu}(\text{H}_2\text{O})_6^{2+}$ (Fig. 2). It is known that $\text{Cu}(\text{H}_2\text{O})_6^{2+}$ shows the Jahn-Teller distortion effect
283 (Sherman, 2001; Bersuker, 2006). Two Cu-O distances of the vertical axial bond
284 (Cu-O_{ax}) are longer than four Cu-O distances in the equatorial plane (Cu-O_{eq}). The
285 Jahn-Teller effect lowers the symmetry of $\text{Cu}(\text{H}_2\text{O})_6^{2+}$ from octahedral T_h to D_{2h} . The
286 calculated bond distance of Cu-O and the literature values are shown in Table 3. The
287 bond distances were calculated to be 2.02-2.03 Å (Cu-O_{eq}) and 2.30 Å (Cu-O_{ax}), which
288 are consistent with those reported in the literature (see references in Table 3).

289 After evidence was found that the stable aqueous complex has a fivefold
290 coordination (Pasquarello et al., 2001), the Jahn-Teller effect of $\text{Cu}(\text{H}_2\text{O})_6^{2+}$ in aqueous
291 solutions has been questioned (Chaboy et al., 2006). The $\text{Cu}(\text{H}_2\text{O})_5^{2+}$ complex has five
292 identical Cu-O bonds with a length of 1.96 Å, which was identified by neutron
293 diffraction (ND) analysis combined with first-principles molecular dynamics (MD). The
294 common bond distance reflects the rapid switch between the square pyramid and
295 trigonal bipyramid configurations (Pasquarello et al., 2001; de Almeida et al., 2008). In
296 a Car-Parrinello MD simulation (Amira et al., 2005), a square pyramidal geometry with
297 four short (2.00 Å) and one long (2.45 Å) Cu-O bond could be optimized. A similar set
298 of bond distances, four short (1.97 Å) and one long (2.39 Å) Cu-O bond, has been
299 confirmed in an X-ray absorption study (Benfatto et al., 2002). Our calculation of the
300 $\text{Cu}(\text{H}_2\text{O})_5^{2+}$ geometry also resulted in the square pyramid rather than the trigonal
301 bipyramid of Fig. 2 and Table 4.

302 There is no clearly predominant structure among the four-, five-, and six- fold
303 coordinated Cu(II) ions (Chaboy et al., 2006). In the present study, we tested both the
304 coordination numbers five and six. We also tested a coordination number four to
305 evaluate the possibility of steric hindrance and strong degree of covalency. The
306 optimized structures in Cartesian coordinates are given in Table S1 of the electronic
307 supplement.

308 The intramolecular vibrational frequencies were then calculated for aqueous
309 Cu(II) species with optimized geometries. The $\ln \beta [= \ln (s/s')f]$ values for the isotope
310 pair $^{65}\text{Cu}/^{63}\text{Cu}$ were determined by employing Eqs. 2-4 and are listed in Table 5. The
311 value of $\ln \beta$ of $\text{Cu}(\text{H}_2\text{O})_5^{2+}$ at 298 K is 0.26‰ larger than that of $\text{Cu}(\text{H}_2\text{O})_6^{2+}$.

312

313 3.3.2. Hydrated Cu(II) chlorides

314 The structure of the hydrated Cu(II) chloride $\text{CuCl}_m(\text{H}_2\text{O})_n^{2-m}$ is shown in
315 Tables 6 and S1 together with literature values. For the Cu(II) *monochloride*, CuCl^+ ,
316 both fivefold (D'Angelo et al., 1997) and sixfold (Rode and Islam, 1992; Texler et al.,
317 1998) coordination have been reported. The bond distances obtained for the
318 fivefold-coordinated $\text{CuCl}(\text{H}_2\text{O})_4^+$ reproduce the experimental results of D'Angelo et al.
319 (1997). Though the geometry of sixfold-coordinated $\text{CuCl}(\text{H}_2\text{O})_5^+$ was optimized within
320 the SCF convergence criterion, this species still showed a few imaginary (negative)
321 frequencies. Tighter convergence criteria may be needed.

322 The Jahn-Teller effect should be detectable in the sixfold-coordinated Cu(II)
323 *dichloride*, $\text{CuCl}_2(\text{H}_2\text{O})_4$. For a geometry with an axial Cl-Cu-Cl bond, we found two
324 long and two short Cu-O bonds in the equatorial plane (Fig. 2). Our calculation agreed
325 with the bond distances determined experimentally (Neilson, 1982; Tajiri and Wakita,
326 1986). A fivefold coordinated structure was inferred from the experiments of Ansell et
327 al. (1995), and, indeed, we found evidence for a stable fivefold-coordinated
328 $\text{CuCl}_2(\text{H}_2\text{O})_3$ structure with a distorted square pyramid (Fig. 2).

329 The X-ray diffraction study of Bell et al. (1973) reports the existence of
330 sixfold-coordinated Cu(II) *trichloride*, $\text{CuCl}_3(\text{H}_2\text{O})_3^-$, which is an average structure of
331 polymerized Cu(II) chlorides in a concentrated CuCl_2 solution. The complex has three
332 Cu-Cl and three Cu-O bonds, a very low symmetry, and is unstable. The isolated CuCl_3^-
333 anion in solution may have a different structure. There are no reports in the literature of
334 the fivefold-coordinated $\text{CuCl}_3(\text{H}_2\text{O})_2^-$. Convergence could not be achieved for the
335 square pyramidal nor the trigonal bipyramidal geometry. A smaller coordination
336 number was found for hydrated CuCl_3^- (Collings et al., 2000). Under highly

337 concentrated HCl and CuCl₂ conditions, a higher order chlorinated CuCl₄²⁻ exists. It is
 338 disputed whether the structure is distorted octahedral CuCl₄(H₂O)₂²⁻ or tetrahedral
 339 CuCl₄²⁻ (see references in Table 6). Systematic analysis by the extended X-ray
 340 absorption fine structure (EXAFS) technique and Raman spectrometry suggested that a
 341 possible structure is the tetrahedral CuCl₄²⁻ (Tanimizu et al., 2007). This supports the
 342 existence of fourfold-coordinated CuCl₃H₂O⁻. The calculation of CuCl₃H₂O⁻
 343 successfully converged.

344 The ln β values of the hydrated chlorides are shown in Fig. 3 and Table 5. As
 345 for the hydrated Cu²⁺ case, ln β (298 K) of the fivefold-coordinated CuCl₂(H₂O)₃ was
 346 found to be 0.26‰ larger than that of the sixfold-coordinated CuCl₂(H₂O)₄. A
 347 difference of this magnitude is assigned to a stereochemical effect. For the fivefold
 348 coordination, the ln β value at 298 K for Cu(H₂O)₅²⁺ is 0.56‰ larger than that of
 349 CuCl₂(H₂O)₃ (Table 5). Likewise, for the sixfold coordination, the ln β value at 298 K
 350 for Cu(H₂O)₆²⁺ is also 0.56‰ larger than that of CuCl₂(H₂O)₄ (Table 5). This suggests
 351 that, with the same coordination number, exchanging H₂O by Cl⁻ enhances ⁶⁵Cu/⁶³Cu
 352 fractionation by approximately the same amount.

353

354 As shown in Fig. 3, ln β decreases when the fraction of H₂O exchanged with
 355 Cl⁻ increases. The variation of Δ⁶⁵Cu estimated from the ln β values (298 K) with the
 356 molarity of HCl is shown in Fig. 1b. A similar observation was previously made for Ni
 357 and Zn isotope fractionation (Fujii et al., 2010, 2011a).

358 The isotopic mass balance is preserved in the extraction system as,

$$\frac{\Sigma[{}^{65}\text{Cu}]}{\Sigma[{}^{63}\text{Cu}]} = \frac{[{}^{65}\text{Cu}^{2+}] + [{}^{65}\text{CuCl}^+] + [{}^{65}\text{CuCl}_2] + [{}^{65}\text{CuCl}_3^-] + [{}^{65}\text{CuLCl}_2]}{[{}^{63}\text{Cu}^{2+}] + [{}^{63}\text{CuCl}^+] + [{}^{63}\text{CuCl}_2] + [{}^{63}\text{CuCl}_3^-] + [{}^{63}\text{CuLCl}_2]} \quad (13)$$

359

360 The mole fractions of related Cu(II) species are evaluated from the values of K_{CuCl^+} ,
361 K_{CuCl_2} , $K_{CuCl_3^-}$ (Brugger, 2001), and D (Eq. 11), all obtained experimentally. Each mole
362 fraction is the sum of fractions of ^{63}Cu and ^{65}Cu isotopologues. The isotopic fractions
363 within the species were estimated from $\ln \beta$. Since there is no structural information of
364 the Cu-DC18C6 complex in organic solution, β_{CuLCl_2} was set as a free parameter. The
365 results of the calculation are shown in Fig. 1b. The value of $\ln \beta_{CuLCl_2}$ converged to
366 3.35‰. The bold and dotted curves shown in Fig. 1b are the values of $\Delta^{65}\text{Cu}$ calculated
367 for $\ln \beta_{CuLCl_2} = 3.35 \pm 0.05\text{‰}$. The results agree well with the experimental results. An
368 important aspect of the estimation is that the calculation correctly predicts the sigmoidal
369 dependence of $\ln \beta$ on the fraction of H_2O exchanged by Cl^- with increasing HCl
370 molarity.

371

372 **3.4. Application to hydrous geochemistry**

373 In the absence of organic ligands which are known to dominate Cu speciation
374 in seawater (Moffet, 1995; Moffet and Brand, 1996; Hirose, 2006) the free Cu^{2+} ion is
375 dominant in freshwater, while the carbonate complexes CuCO_3 and $\text{Cu}(\text{CO}_3)_2^{2-}$ are
376 dominant in seawater (Albarède, 2004). Copper concentration in seawater increase
377 down the water column, which indicates both the uptake of Cu by plankton and
378 scavenging of Cu by settling particles (Boyle et al., 1977; Bruland, 1980). Dissolved Cu
379 in seawater is isotopically heavy ($\delta^{65}\text{Cu} = +0.9$ to $+1.5\text{‰}$) relative to rocks and
380 sediments (0.0 to $+0.3\text{‰}$) and the riverine input ($+0.69\text{‰}$) (Bermin et al., 2006; Vance
381 et al., 2008). It was suggested that this result is attributable to the partitioning of Cu

382 isotopes between a heavy dissolved phase, where Cu is bound to organic ligands, and a
383 light particulate phase, dominated by Fe-Mn oxides (Vance et al., 2008). $\delta^{65}\text{Cu}$ in
384 Fe-Mn nodules (Albarède, 2004) and encrustations (Little et al., 2010) from the three
385 major ocean basins varies between +0.04 and +0.6‰, which is significantly lighter than
386 the $\delta^{65}\text{Cu}$ value in seawater (+0.9 to +1.5‰, Vance et al., 2008).

387 Surface seawater also contains various inorganic complexes and carbonates.
388 Speciation of Cu in seawater is very sensitive to the hydrolysis constants. Zirino and
389 Yamamoto (1972) used the cumulative formation constant of $\text{Cu}(\text{OH})_2$, $\log \beta_2 = 14.3$,
390 which, as shown in Fig. S1a (see the electronic supplement), makes Cu speciation in
391 seawater dominated by $\text{Cu}(\text{OH})_2$. Mole fractions have been calculated from the set of
392 stability constants recommended by Powell et al. (2007) with the second hydrolysis
393 constant $\log \beta_2 = -16.65$, and the results are shown in Fig. 4a as a function of pH. At a
394 typical seawater pH of 8.22 (Macleod et al., 1994), CuCO_3 is the dominant species,
395 while the hydrated Cu^{2+} ion, chloride, sulfate, and hydroxide are subordinate. At $\text{pH} \geq$
396 8.22, $\text{Cu}(\text{CO}_3)_2^{2-}$ becomes an abundant species. These calculations are only relevant to
397 seawater with no organic ligands.

398 Figure 4b shows the isotope fractionation of Cu(II) among its various species
399 as estimated from their mole fractions and $\ln \beta$ (Tables 5 and 7) at 298 K under
400 conditions typical of seawater. The optimized geometries of the relevant species are
401 shown in Fig. 2 and Table S1 and the temperature dependence of $\ln \beta$ (Table 7) in Fig. 5.
402 The geometry of Cu hydroxides, CuOH^+ and $\text{Cu}(\text{OH})_2$, were calculated by dissociating
403 H^+ ions from the *fivefold*-coordinated $\text{Cu}(\text{H}_2\text{O})_5^{2+}$. The positions of OH^- ligands were
404 determined by reference to CuCl^+ and CuCl_2 (Fig. 2). The structure calculated for both

405 $\text{CuOH}(\text{H}_2\text{O})_4^+$ and $\text{Cu}(\text{OH})_2(\text{H}_2\text{O})_3$ converged to a distorted square pyramid. With a
406 H_2O molecule at the vertex of the square pyramid, the bond distance is shorter for
407 $\text{Cu}-\text{OH}^-$ (1.8-1.9 Å) than for $\text{Cu}-\text{OH}_2$ (2.3-2.4 Å) (see Table S1). This suggests that the
408 stronger Cu-O bonds on the square plane loosen the hydration bond from the vertex.
409 This conclusion is consistent with the known structure of amorphous $\text{Cu}(\text{OH})_2$ or
410 $\text{Cu}(\text{OH})_2$ colloidal solution, which both show a layer structure of polymerized square
411 planes (Elizarova et al., 1999; Kriventsov et al., 1999).

412 *Fourfold* complexation occurs in both amorphous and crystalline $\text{Cu}(\text{OH})_2$. A
413 stable fourfold complexation was also obtained for the Cu(II) carbonates, $\text{CuCO}_3(\text{H}_2\text{O})_2$
414 and $\text{Cu}(\text{CO}_3)_2^{2-}$ (Fig. 2 and Table S1). CO_3^{2-} was treated as a bidentate ligand. The
415 structure converged to a distorted square plane. We tested positioning a water molecule
416 above the plane in the initial structure, but it moved out of the inner coordination shell
417 during the calculation. The structural optimization of CuCO_3OH^- was more problematic.
418 Since CO_3^{2-} and OH^- occupy three coordination positions, one water molecule should
419 also bind to Cu(II) at the fourth coordination position, thereby giving the
420 $\text{CuCO}_3(\text{OH})\text{H}_2\text{O}^-$ compound. It was actually found that no water molecule is stable in
421 the inner coordination shell. From the stoichiometry, the stable model molecule may
422 instead be $\text{CuHCO}_3(\text{OH})_2^-$. This stable structure, in which HCO_3^- acts as a
423 quasi-bidentate ligand is shown in Fig. 2 and Table S1. The $\ln \beta$ values obtained are
424 shown in Fig. 5 and Table 7. The Cu hydroxides and carbonates have $\ln \beta$ values of
425 4.3-5.2‰ (298 K), in which compounds with higher complexation with OH^- and CO_3^{2-}
426 resulted in $\ln \beta \geq 5\text{‰}$ (298 K).

427 The structure of hydrated Cu(II) in sulfate solutions was previously
428 investigated by Ohtaki et al. (1976) and Musinu et al. (1983). In CuSO_4 solutions, Cu^{2+}

429 is surrounded by disordered ligands (Musinu et al., 1983), which suggests a direct
430 interaction of Cu^{2+} with SO_4^{2-} . We used the structural model of Fe(III) sulfate proposed
431 by Magini (1979) as a reference for $\text{CuSO}_4(\text{H}_2\text{O})_4$ (Fig. 2 and Table S1), in which SO_4^{2-}
432 is treated as a monodentate ligand, and obtained bond distances of 1.9-2.1 Å for
433 Cu-OH_2 and 2.37 Å for Cu-OSO_3^{2-} . These values agree with the Cu-O bond distances
434 determined by X-ray diffraction (Musinu et al., 1983). The electron donor SO_4^{2-}
435 strongly attracts H^+ and the resulting structure is equivalent to $\text{CuH}_2\text{SO}_4(\text{OH})_2$ (Fig. 2).
436 The magnitude of $\ln \beta$ for CuSO_4 is 5.14‰ at 298 K (Table 7) and matches that of
437 $\text{Cu}(\text{CO}_3)_2^{2-}$ (Fig. 5).

438 As shown in Figs. 4a and 4b, at $\text{pH} \geq 8.22$, the dominant Cu(II) species are
439 carbonates. We found that Cu in $\text{Cu}(\text{CO}_3)_2^{2-}$ (and CuSO_4) is isotopically 0.6‰ heavier
440 than Cu^{2+} ion. At $\text{pH} = 8.22$, the $\delta^{65}\text{Cu}$ value of CuCO_3 is slightly negative -0.17‰ ,
441 whereas those of $\text{Cu}(\text{CO}_3)_2^{2-}$ and CuCO_3OH^- are substantially heavier, 0.75‰ and
442 0.58‰, respectively. At high pH, the relevant fractionation factors are
443 $\Delta^{65}\text{Cu}[\text{Cu}(\text{CO}_3)_2^{2-}-\text{CuCO}_3] = 0.92\text{‰}$ and $\Delta^{65}\text{Cu}[\text{CuCO}_3\text{OH}^--\text{CuCO}_3] = 0.75\text{‰}$. Copper
444 in carbonates, whether in CuCO_3 or in solid solutions with carbonates of other elements
445 should therefore be isotopically light with respect to dissolved Cu.

446 At $\text{pH} = 8.22$, $\text{Cu}(\text{OH})_2$ is $+0.48\text{‰}$ heavier than bulk seawater Cu (Fig. 4b). A
447 caveat is the somewhat different fractionation obtained when the cumulative formation
448 constant of $\text{Cu}(\text{OH})_2$, $\log \beta_2 = 14.3$ of Zirino and Yamamoto (1972) is used. The major
449 species are $\text{Cu}(\text{OH})_2$ and CuCO_3 , while mole fractions of other species are insignificant
450 (Fig. S1a, Zirino and Yamamoto, 1972). The $\delta^{65}\text{Cu}$ shift of $\text{Cu}(\text{OH})_2$ and CuCO_3 at pH
451 $= 8.22$ with respect to dissolved Cu are $+0.02\text{‰}$ and -0.62‰ , respectively (Fig. S1b).

452 Isotope fractionation may therefore not be seen in Cu(II) hydroxide, but Cu in CuCO₃
453 should nevertheless remain isotopically light with respect to the seawater value.

454 As sulfides have small $\ln \beta$ values (Fujii et al., 2011b; Pons et al., 2011),
455 sulfate-sulfide and carbonate-sulfide exchange are possibly determinant reactions for Cu
456 isotope fractionation in seawater. CuHS(H₂O)₄⁺ and Cu(HS)₂(H₂O)₃ were calculated
457 with the geometries shown in Table S1. The structures that successfully converged were
458 similar to those of the hydroxides shown in Fig. 2. The $\ln \beta$ values are shown in Fig 5
459 and Table 7. It is clear that the $\ln \beta$ values of Cu(II) sulfides are smaller than those of all
460 the species shown in Fig. 3. In particular, the $\ln \beta$ values of Cu sulfides are 1.9-2.0‰
461 smaller than those of Cu sulfate and carbonates. Diagenetic Cu(II)-bearing sulfides are
462 expected to be isotopically lighter than dissolved Cu, while Cu in the water table of
463 sulfide-rich terranes should be heavy (Mathur et al., 2005, 2012).

464 Isotope fractionation also occurs under reducing conditions through
465 Cu(I)-Cu(II) redox reactions. The $\ln \beta$ values calculated for Cu(I) chlorides and
466 hydrogensulfides are $\leq 2.6\text{‰}$ at 298 K (Seo et al., 2007), which suggests that Cu(I)
467 complexes preferentially enrich ⁶³Cu and their precipitation results in the enrichment of
468 ⁶⁵Cu in the fluid.

469 Cu in sulfides should be isotopically light with respect to dissolved aqueous Cu,
470 and the main form of Cu removal from aquatic systems is Cu sulfide. The heavy
471 isotopic composition of Cu in surface seawater (Vance et al., 2008) and groundwater
472 (Mathur et al., 2012) therefore likely reflects that Cu carbonate complexes are held back
473 in solution, while Cu is precipitated in sulfides. Complexation of Cu(II) with organic
474 matter in surface seawater (Moffett, 1995) should also cause Cu isotope fractionation.

475 Evidence for the large-scale deposition of sediments with isotopically light Cu required
476 by mass balance is, however, still missing.

477

478 **3.5. Application to biological activity**

479 A variety of biological processes may induce Cu isotope fractionation.
480 Pokrovsky et al. (2008) demonstrated that Cu in bacteria is isotopically light relative to
481 the ambient solution. Pokrovsky et al. (2012) further identified S-coordinated Cu(I)
482 complexes at the surface and inside bacterial cells that may preferentially concentrate
483 ^{63}Cu over ^{65}Cu . It is therefore appealing to assign isotope fractionation in biological
484 material to competing Cu(II) and Cu(I) complexation. Mammal physiology is also a
485 cause of Cu isotope fractionation. Albarede et al. (2011a) found a $\sim 1\text{‰}$ fractionation
486 between human erythrocytes and serum. High $\delta^{65}\text{Cu}$ values of 1.5‰ were found in the
487 kidney of both sheep (Balter and Zazzo, 2011) and mice (Albarède et al., 2011b) with
488 respect to the rest of the body.

489 Oxalic acid is an ubiquitous toxic organic acid in body fluids. Oxalate is
490 adsorbed in the intestinal track, but the question of the origin of high oxalate contents in
491 urine and plasma found in patients prone to kidney damage is still contentious. This is a
492 genuine medical concern as ascorbate (vitamin C) supplementation has been argued to
493 increase the urinary oxalate levels, and therefore ascorbate may be a risk factor for
494 individuals predisposed to kidney stones (Chai et al., 2005; González et al., 2005;
495 Massey et al., 2005). Ascorbate is efficiently converted to oxalate when the coexisting
496 copper concentration is high (Hayakawa et al., 1973).

497 Hayakawa et al. (1973) suggest that Cu(II) is readily reduced by ascorbic acid
498 (H_2A) to Cu(I),



499

500 The ascorbate anion A^{2-} here is oxidized to A, dehydroascorbic acid $\text{C}_6\text{H}_6\text{O}_6$. In the
 501 catalytic reaction by a multicopper oxidase, ascorbate oxidase, the oxidation of
 502 ascorbate to dehydroascorbate occurs via the disproportionation of the
 503 semidehydroascorbate radical (Solomon et al., 1996). The enzymatic reactions may be
 504 identical to the catalytic reaction 14.

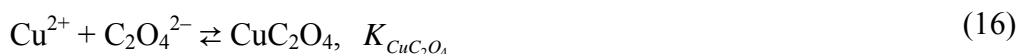
505 The monohydroascorbate anion HA^- forms a complex with Cu^{2+} , CuHA^+ .



506

507 Degradation of ascorbate via dehydroascorbate forms oxalate. A pathway of ascorbate
 508 degradation has been proposed by Green and Fry (2005).

509 The oxalic acid also forms a complex with Cu^{2+} , CuC_2O_4 .



510

511 The value of the standard redox potential Eh with respect to the standard hydrogen
 512 electrode (SHE), E_0 , for the Cu redox reaction,



513

514 is $E_0 = 0.153 + 0.591 \log ([\text{Cu}^{2+}]/[\text{Cu}^+])$ (Pourbaix, 1974). We used the following acid
 515 dissociation constants and equilibrium constants $\text{p}K_a = 4.03$ (ascorbic acid), $\text{p}K_{a1} =$
 516 1.252 , $\text{p}K_{a2} = 4.266$ (oxalic acid) (Smith and Martell, 1989), $\log K_{\text{CuHA}^+} = 2.32$

517 (Jameson et al., 1976), and $\log K_{\text{CuC}_2\text{O}_4} = 4.5$ (Foreci et al., 1995). Figure 6a shows the
518 mole fractions of Cu^+ , Cu^{2+} , CuHA^+ , and CuC_2O_4 as functions of Eh. The total
519 concentrations of Cu and ascorbic acid are $\sim 10^{-6}$ M (Lech and Sadlik, 2007) and $\sim 10^{-4}$
520 M (Margolls and Davis, 1988), respectively. The pH and Eh in the body are known to
521 be ~ 7.4 and 0.27 V (van Rossum and Schamhart, 1991). These values were used to
522 estimate the mole fractions of Cu species using the assumption that 10% of ascorbic
523 acid is converted to oxalic acid. We further assumed that no other degradation products
524 were present. Figure 6b shows the speciation as a function of the reaction progress. As
525 expected, oxidation of Cu(I) to Cu(II) proceeds with increasing Eh, which in turn
526 enhances Cu-ascorbate and Cu-oxalate formation. The degradation of ascorbate
527 increases oxalic acid concentration and therefore promotes the production of
528 Cu-oxalate.

529 Figure 6c and 6d show the range of isotope fractionation among Cu species as
530 estimated from their mole fractions and $\ln \beta$ at 298 K (Tables 5 and 8). The optimized
531 geometries of related species are shown in Table S1. Hydrated Cu^+ was treated as free
532 Cu(I). Cu(I) complexes possess simple linear structures (Fulton et al., 2000a,b). Our \ln
533 β value of 2.87‰ at 289K for $\text{Cu}(\text{H}_2\text{O})_2^+$ (Table 8) is consistent with the value of
534 2.89‰ estimated by *ab initio* methods for CuClH_2O (Seo et al., 2007). $\text{Cu}(\text{H}_2\text{O})_5^{2+}$ was
535 treated as free Cu(II), and its $\ln \beta$ is given in Table 5. For the geometry of Cu(II)
536 ascorbate CuHA^+ , we used the copper monomer (Ünaleroğlu et al., 2001). The structure
537 calculated for Cu(II) in fivefold coordination with L-ascorbate and H_2O is shown in Fig.
538 2 and Table S1. The value of $\ln \beta$ calculated at 298 K is 3.32‰. The $\ln \beta$ value of
539 D-ascorbate at 298 K (also 3.38‰) is indistinguishable from that of L-ascorbate. The

540 geometry of Cu(II) oxalate was quite similar to the structure of the hydrated Cu
541 carbonate. It successfully converged to a distorted plane configuration (Fig. 2 and Table
542 S1) and led to large $\ln \beta$ values (Fig.7 and Table 8).

543 Figures 6c and 6d show the $\delta^{65}\text{Cu}$ values of the different species relative to the
544 bulk solution as a function of Eh and extent of oxalate formation. Figure 6c shows that,
545 with respect to free Cu(II), free Cu(I) is enriched in the light isotope. When Cu(I) and
546 Cu(II) coexist, the $\delta^{65}\text{Cu}$ of the total free Cu ions is only slightly lighter than the sum of
547 all the Cu species. The $\delta^{65}\text{Cu}$ of the Cu ascorbate varies from -1.0 to $+0.5\text{‰}$ when Eh
548 increases from -1 V to $+1$ V, but its mole fraction remains very small. The prominent
549 feature of Fig. 6c is the heavy isotope enrichment ($+0.6$ to $+2.5\text{‰}$) of the Cu oxalate
550 relative to total Cu. Figure 6d was drawn for Eh = 0.27 V, which is a typical Eh value of
551 human blood. It is expected that degradation of ascorbate and excretion of oxalate
552 should leave isotopically heavy Cu in the kidney. With respect to food, which has a
553 $\delta^{65}\text{Cu}$ value of about 0‰ (Balter and Zazzo, 2011), when even trace amounts of oxalate
554 form, it should leave behind copper with a $\delta^{65}\text{Cu}$ of $\sim 1.4\text{‰}$. This value is very close to
555 the $\delta^{65}\text{Cu}$ (of 1.5‰) found in sheep (Balter and Zazzo, 2011) and mice (Albarède et al.,
556 2011b) kidneys. The positive $\delta^{65}\text{Cu}$ found in kidneys may result from isotopically heavy
557 Cu left in the kidney by the degradation of ascorbic acid. Copper isotopes therefore
558 represent a potential marker of the troubles associated with hyperoxalury and kidney
559 stones.

560

561

4. CONCLUSIONS

562 We first demonstrated that Cu isotope fractionation at equilibrium is observed in
563 laboratory-scale experiments. The effect on the $^{65}\text{Cu}/^{63}\text{Cu}$ ratio of Cu(II) partitioning
564 between HCl and DC18C6 depends on acid molarity. The effect is mainly governed by
565 the mass-dependent fractionations as a result of intramolecular vibrations. The nuclear
566 field shift effect accounts for less than 3% of the mass-dependent fractionation. We then
567 computed the coefficients of isotope fractionation of Cu for several species (hydrated
568 Cu ion, hydroxide, chloride, sulfide, sulfate, carbonate, oxalate, and ascorbate). It was
569 found that Cu in dissolved carbonates and sulfates is isotopically heavier than free Cu
570 and Cu in sulfides. The theoretical estimation of $\delta^{65}\text{Cu}$ in ligand exchange between
571 inorganic ligands including carbonate anions may be useful to understand the heavy Cu
572 isotopic compositions found in both seawater and groundwater in the absence of strong
573 organic ligands. Further theoretical estimation of $\delta^{65}\text{Cu}$ in hydrated Cu(I) and Cu(II)
574 ions, Cu(II) ascorbates, and Cu(II) oxalate suggests that Cu isotope fractionation during
575 the breakdown of ascorbate into oxalate results in the isotopically heavy Cu found in
576 mammal kidneys.

577

578

ACKNOWLEDGMENT

579

580

581

582

583

584

The authors thank the anonymous reviewers and Associate Editor Mark
Rehkämper for their useful suggestions and constructive comments on the manuscript.
The authors wish to thank the generous help of Janne Blichert-Toft in editing the
English of this paper. FM acknowledged the support of NASA EXO (NNX12AD88G)
and of the Washington University I-CARES program.

585 **REFERENCES**

- 586 Abe M., Suzuki T., Fujii Y., Hada M. and Hirao K. (2008) An *ab initio* molecular
587 orbital study of the nuclear volume effects in uranium isotope fractionations. *J. Chem.*
588 *Phys.* **129**, 164309.
- 589 Abe M., Suzuki T., Fujii Y., Hada M., Hirao K. (2010) Ligand effect on uranium
590 isotope fractionations caused by nuclear volume effects: An *ab initio* relativistic
591 molecular orbital study. *J. Chem. Phys.* **133**, 044309.
- 592 Åkesson R., Pettersson L. G. M., Sandström M. and Wahlgren U. (1992) Theoretical
593 calculations of the Jahn-Teller effect in the hexahydrated copper(II), chromium(II),
594 and manganese(III) ions, $[\text{Cu}(\text{H}_2\text{O})_6]^{2+}$, $[\text{Cr}(\text{H}_2\text{O})_6]^{2+}$, and $[\text{Mn}(\text{H}_2\text{O})_6]^{3+}$, and
595 comparisons with the hexahydrated copper(I), chromium(III), and manganese(II)
596 clusters. *J. Phys. Chem.* **96**, 150-156.
- 597 Albarède F. (2004) The stable isotope geochemistry of copper and zinc. *Rev. Mineral.*
598 *Geohem.* **55**, 409-427.
- 599 Albarède F., Telouk P., Lamboux A., Jaouen K. and Balter V. (2011a) Isotopic evidence
600 of unaccounted for Fe and Cu erythropoietic pathways. *Metallomics* **3**, 926-933.
- 601 Albarède F., Balter V., Jaouen K. and Lamboux A. (2011b) Applications of the stable
602 isotopes of metals to physiology. *The 38th Meeting of the Federation of Analytical*
603 *Chemistry and Spectroscopy Societies (FACSS)*, Reno (abstract).
- 604 Amira S., Spångberg D. and Hermansson K. (2005) Distorted five-fold coordination of
605 $\text{Cu}^{2+}(\text{aq})$ from a Car-Parrinello molecular dynamics simulation. *Phys. Chem. Chem.*
606 *Phys.* **7**, 2874-2880.
- 607 Angeli I. (2004) A consistent set of nuclear rms charge radii: properties of the radius
608 surface $R(N,Z)$. *At. Data Nucl. Data Tables* **87**, 185-206.

609 Ansell S., Tromp R. H. and Neilson G. W. (1995) The solute and aquaion structure in a
610 concentrated aqueous solution of copper(II) chloride. *J. Phys.: Condens. Matter* **7**,
611 1513-1524.

612 Archer C. and Vance D. (2002) Mass discrimination correction in multiple collector
613 plasma source mass-spectrometry: an example using Cu and Zn isotopes. *J. Anal. At.*
614 *Spectrom.* **64**, 356-365.

615 Balistrieri L. S., Borrok D. M., Wanty R. B. and Ridley W. I. (2008) Fractionation of
616 Cu and Zn isotopes during adsorption onto amorphous Fe(III) oxyhydroxide:
617 Experimental mixing of acid rock drainage and ambient river water. *Geochim.*
618 *Cosmochim. Acta* **72**, 311-328.

619 Balter V. and Zazzo A. (2011) An animal model (sheep) for Fe, Cu, and Zn isotopes
620 cycling in the body. *Mineralogical Magazine* **75**, 476-476.

621 Beagley B., Eriksson A., Lindgren J., Persson I, Pettersson L. G. M., Sandström M.,
622 Wahlgren U. and White E. W. (1989) A computational and experimental study on
623 the Jahn-Teller effect in the hydrated copper (II) ion. Comparisons with hydrated
624 nickel (II) ions in aqueous solution and solid Tutton's salts. *J. Phys.: Condens. Matter*
625 **1**, 2395-2408.

626 Becke A. D. (1993) Density-functional thermochemistry. 3. The role of exact exchange.
627 *J. Chem. Phys.* **98**, 5648-5652.

628 Benfatto M., D'Angelo P., Della Longa S. and Pavel N. V. (2002) Evidence of distorted
629 fivefold coordination of the Cu²⁺ aqua ion from an x-ray-absorption spectroscopy
630 quantitative analysis. *Phys. Rev. B* **65**, 174205.

631 Bell J. R., Tyvoll J. L. and Wertz D. L. (1973) Solute structuring in aqueous copper(II)
632 chloride solutions. *J. Am. Chem. Soc.* **95**, 1456-1459.

- 633 Ben Othman D., Luck J. M., Bodinier J. L., Arndt N. T. and Albarède F. (2006) Cu-Zn
634 isotopic variations in the Earth's mantle. *Geochim. Cosmochim. Acta Suppl.* **70**,
635 46-46.
- 636 Bermin J., Vance D., Archer C. and Statham P.J. (2006) The determination of the
637 isotopic composition of Cu and Zn in seawater. *Chem. Geol.* **226**, 280-297.
- 638 Bersuker I. B. (2006) *The Jahn-Teller effect*; Cambridge Univ. Press, New York.
- 639 Bigalke M., Weyer S. and Wilcke W. (2010) Stable copper isotopes: a novel tool to
640 trace copper behavior in hydromorphic soils. *Soil Sci. Soc. Am. J.* **74**, 60-73.
- 641 Bigalke M., Weyer S. and Wilcke W. (2011) Stable Cu isotope fractionation in soils
642 during oxic weathering and podzolization. *Geochim. Cosmochim. Acta* **75**,
643 3119-3134.
- 644 Bigeleisen J. and Mayer M. G. (1947) Calculation of equilibrium constants for isotopic
645 exchange reactions. *J. Chem. Phys.* **15**, 261-267.
- 646 Bigeleisen J. (1996) Nuclear size and shape effects in chemical reactions. isotope
647 chemistry of the heavy elements. *J. Am. Chem. Soc.* **118**, 3676-3680.
- 648 Bishop M. C., Moynier F., Weinsten C., Fraboulet J. G., Wang K. and Foriel J. (2012)
649 Cu isotopic composition of iron meteorites. *Meteor. Planet. Sci.* **47**, 268-276.
- 650 Black J. R., Kavner A. and Schauble E. A. (2011) Calculation of equilibrium stable
651 isotope partition function ratios for aqueous zinc complexes and metallic zinc.
652 *Geochim. Cosmochim. Acta* **75**, 769-783.
- 653 Boyle E. A., Sclater F. R. and Edmond J.M. (1977) The distribution of dissolved copper
654 in the Pacific. *Earth Planet. Sci. Lett.*, **37**, 38-54.
- 655 Breza M., Biskupic S. and Kozisek J. (1997) On the structure of hexaaquacopper(II)
656 complex. *J. Mol. Struct. (Teochem)* **397**, 121-128.

657 Brugger J., McPhail D. C., Black J and Spiccia L. (2001) Complexation of metal ions in
658 brines: application of electronic spectroscopy in the study of the Cu(II)-LiCl-H₂O
659 system between 25 and 90°C. *Geochim. Cosmochim. Acta* **65**, 2691.

660 Bruland K.W. (1980) Oceanographic distributions of cadmium, zinc, nickel, and copper
661 in the North Pacific. *Earth Planet. Sci. Lett.* **47**, 176-198.

662 Bryantsev V. S., Diallo M. S., van Duin A. C. T. and Goddard III W. A. (2008)
663 Hydration of copper(II): new insights from density functional theory and the COSMO
664 solvation model. *J. Phys. Chem. A* **112**, 9104-9112.

665 Chaboy J., Muñoz-Páez A., Merklings P. J. and Sánchez Marcos E. (2006) The hydration
666 of Cu²⁺: Can the Jahn-Teller effect be detected in liquid solution? *J. Chem. Phys.* **124**,
667 064509.

668 Chai W., Liebman M., Kynast-Gales S. and Massey L. (2004) Oxalate absorption and
669 endogenous oxalate synthesis from ascorbate in calcium oxalate stone formers and
670 non-stone formers. *Am. J. Kidney Diseases* **44**, 1060-1069.

671 Collings M. D., Sherman D. M. and Ragnarsdottir K. V. (2000) Complexation of Cu²⁺
672 in oxidized NaCl brines from 25°C to 175°C: results from in situ EXAFS
673 spectroscopy. *Chem. Geol.* **167**, 65-73.

674 Contreras F., Fontal B. and Bianchi G. (1993) Copper(II) thiocyanide complexes
675 extractable with [dibenzo-18-crown-6-K]⁺ in chloroform. *Transition Met. Chem.* **18**,
676 104-106.

677 Cowan J.A. (1997) *Inorganic Biochemistry*, Wiley-VCH, New York.

678 de Almeida K. J., Murugan N. A., Rinkevicius Z., Hugosson H. W., Vahtras O., Ågren
679 H. and Cesar A. (2009) *Phys. Chem. Chem. Phys.* **11**, 508-519.

680 de Bruin T. J. M., Marcelis A. T. M., Zuilhof H. and Sudhölter E. J. R. (1999)
681 Geometry and electronic structure of bis-(glycinato)-Cu^{II}·2H₂O complexes as studied
682 by density functional B3LYP computations. *Phys. Chem. Chem. Phys.* **1**, 4157-4163.

683 Dennington R., Keith T. and Millam J. (2009) *GaussView, Version 5.0.8*. Semichem
684 Inc., Shawnee Mission KS.

685 Eigen M. (1963) Fast elementary steps in chemical reaction mechanisms. *Pure Appl.*
686 *Chem.* **6**, 97-116.

687 Elizarova G. L., Kochubey D. I., Kriventsov V. V., Odegova G. V., Matvienko H. L. G.,
688 Kolomyichuk V. N. and Parmon V. N. (1999) Study of the interaction products of
689 some N- and O-containing compounds with highly dispersed copper(II) hydroxide. *J.*
690 *Colloid Interface Sci.* **213**, 126-132.

691 Epov V. N., Malinovskiy D., Vanhaecke F., Begue D. and Donard O. F. X. (2011)
692 Modern mass spectrometry for studying mass-independent fractionation of heavy
693 stable isotopes in environmental and biological sciences. *J. Anal. At. Spectrom.* **26**,
694 1142-1156.

695 Epov V. N (2011) Magnetic isotope effect and theory of atomic orbital hybridization to
696 predict a mechanism of chemical exchange reactions. *Phys. Chem. Chem. Phys.* **13**,
697 13222-13231.

698 Faegri K. (2001) Relativistic Gaussian basis sets for the elements K-Uuo. *Theo. Chem.*
699 *Acc.* **105**, 252-258.

700 Feroci G., Fini A., Fazlo G. and Zuman P. (1995) Interaction between dihydroxy bile
701 salts and divalent heavy metal ions studied by polarography. *Anal. Chem.* **67**,
702 4077-4085.

703 Freeman H. C. and Guss J. M. (2001) Plastocyanin. In *Handbook of Metalloproteins*
704 (eds. R. Huber, T. L. Poulos, and K. Wieghardt), Wiley, Chichester. pp. 1153-1169.

705 Frisch M. J., Trucks G. W., Schlegel H. B., Scuseria G. E., Robb M. A., Cheeseman J.
706 R., Scalmani G., Barone V., Mennucci B., Petersson G. A., Nakatsuji H., Caricato M.,
707 Li X., Hratchian H. P., Izmaylov A. F., Bloino J., Zheng G., Sonnenberg J. L., Hada
708 M., Ehara M., Toyota K., Fukuda R., Hasegawa J., Ishida M., Nakajima T., Honda Y.,
709 Kitao O., Nakai H., Vreven T., Montgomery Jr. J. A., Peralta J. E., Ogliaro F.,
710 Bearpark M., Heyd J. J., Brothers E., Kudin K. N., Staroverov V. N., Kobayashi R.,
711 Normand J., Raghavachari K., Rendell A., Burant J. C., Iyengar S. S., Tomasi J.,
712 Cossi M., Rega N., Millam N. J., Klene M., Knox J. E., Cross J. B., Bakken V.,
713 Adamo C., Jaramillo J., Gomperts R., Stratmann R. E., Yazyev O., Austin A. J.,
714 Cammi R., Pomelli C., Ochterski J. W., Martin R. L., Morokuma K., Zakrzewski V.
715 G., Voth G. A., Salvador P., Dannenberg J. J., Dapprich S., Daniels A. D., Farkas Ö.,
716 Foresman J. B., Ortiz J. V., Cioslowski J. and Fox D. J. (2009) *Gaussian 09, Revision*
717 *B.01*, Gaussian, Inc., Wallingford CT.

718 Fujii T., Moynier F., Telouk P. and Albarede F. (2006) Isotope fractionation of iron(III)
719 in chemical exchange reactions using solvent extraction with crown ether. *J. Phys.*
720 *Chem. A* **110**, 11108-11112.

721 Fujii T., Moynier F. and Albarède F. (2009) The nuclear field shift effect in chemical
722 exchange reactions. *Chem. Geol.* **267**, 139-156.

723 Fujii T., Moynier F., Telouk P. and Abe, M. (2010) Experimental and theoretical
724 investigation of isotope fractionation of zinc between aqua, chloro, and macrocyclic
725 complexes. *J. Phys. Chem. A* **114**, 2543-2552.

726 Fujii T., Moynier F., Dauphas N. and Abe M. (2011a) Theoretical and experimental
727 investigation of nickel isotopic fractionation in species relevant to modern and
728 ancient oceans. *Geochim. Cosmochim. Acta* **75**, 469-482.

729 Fujii T., Moynier F., Pons M. L. and Albarède F (2011b) The origin of Zn isotope
730 fractionation in sulfides. *Geochim. Cosmochim Acta* **75**, 7632-7643.

731 Fujii T., Moynier F., Agranier A., Ponzevera E. and Abe M. (2011c) Nuclear field shift
732 effect of lead in ligand exchange reaction using a crown ether. *Proc. Radiochim. Acta.*
733 **1**, 387-392.

734 Fujii T., Moynier F., Agranier A., Ponzevera E. and Abe M. (2011d) Isotope
735 fractionation of palladium in chemical exchange reaction. *Proc. Radiochim. Acta.* **1**,
736 339-344.

737 Fujii T. and Albarède F. (2012) Ab initio calculation of the Zn isotope effect in
738 phosphates, citrates, and malates and applications to plants and soil. *PLoS ONE* **7**,
739 e30726.

740 Fulton J. L., Hoffmann M. M. and Darab J. G. (2000a) An x-ray absorption fine
741 structure study of copper(I) chloride coordination structure in water up to 325°C.
742 *Chem. Phys. Lett.* **330**, 300-308.

743 Fulton J. L., Hoffmann M. M., Darab J. G., Palmer B. J. and Stern E. A. (2000b)
744 Copper(I) and copper(II) coordination structure under hydrothermal conditions at
745 325°C: an x-ray absorption fine structure and molecular dynamics study. *J. Phys.*
746 *Chem. A* **104**, 11651-11663.

747 Garcia J., Benfatto M., Notoli C. R., Bianconi A., Fontaine A. and Tolentino H. (1989)
748 The quantitative Jahn-Teller distortion of the Cu²⁺ site in aqueous solution by
749 XANES spectroscopy. *Chem. Phys.* **132**, 295-307.

750 González M. J., Miranda-Massari J. R., Mora E. M., Guzmán A., Riordan N. H.,
751 Riordan H. D., Casciari J. J., Jackson J. A. and Román-Franco A. (2005)
752 Orthomolecular oncology review: Ascorbic acid and cancer 25 years later. *Integr.*
753 *Cancer Ther.* **4**, 32-44.

754 Green M. A. and Fry S. C. (2005) Vitamin C degradation in plant cells via enzymatic
755 hydrolysis of 4-O-oxalyl-L-threonate. *Nature* **433**, 83-87.

756 Hayakawa K., Minami S. and Nakamura S. (1973) Kinetics of the oxidation of ascorbic
757 acid by the copper(II) ion in an acetate buffer solution. *Bull. Chem. Soc. Jpn.* **46**,
758 2788.

759 Herzog G. F., Moynier F. and Albarède F. (2009) Isotopic and elemental abundances of
760 copper and zinc in. lunar basalts, glasses, and soils, a terrestrial basalt, Pele's hairs,
761 and Zagami. *Geochim. Cosmochim. Acta.* **73**, 5884-5904.

762 Hill P. S., Schauble E. A. and Young E. D. (2010) Effects of changing solution
763 chemistry on Fe³⁺/Fe²⁺ isotope fractionation in aqueous Fe-Cl solutions. *Geochim.*
764 *Cosmochim. Acta* **74**, 6669-6689.

765 Hirose K. (2006) Chemical speciation of trace metals in seawater: a review. *Anal. Sci.*
766 **22**, 1055-1063.

767 Jameson R. F. and Blackburn N. J. (1976) Role of copper dimers and the participation
768 of copper(III) in the copper-catalysed autoxidation of ascorbic acid. Part II. Kinetics
769 and mechanism in 0.100 mol dm⁻³ potassium nitrate. *J. Chem. Soc., Dalton* 534-541.

770 Jepson B.E. and Cairns G.A. (1979) Lithium isotope effects in chemical exchange with
771 (2,2,1) cryptand, *MLM-2622*.

772 Jouvin D., Weiss D. J., Mason T. F. M., Hinsinger P. and Benedetti M. F. (2012) Stable
773 isotopes of Cu and reduction at the root surface isotopic fractionation processes.
774 *Environ. Sci. Technol.* **46**, 2652-2660.

775 King W. H. (1984) *Isotope Shifts in Atomic Spectra*; Plenum Press, New York.

776 Klein S., Domergue C., Lahaye Y., Brey G. P. and von Kaenel H.-M. (2009) The lead
777 and copper isotopic composition of copper ores from the Sierra Morena (Spain). *J.*
778 *Iberian Geol.* **35**, 59-68.

779 Koc K. and Ishikawa Y. (1994) Single-Fock-operator method for matrix Dirac-Fock
780 self-consistent-field calculations on open-shell atoms. *Phys. Rev. A* **49**, 794-798.

781 Kriventsov V. V., Kochubey D. I., Elizarova G. L., Matvienko H. L. G. and Parmon V.
782 N. (1999) The structure of amorphous bulk and silica-supported copper(II)
783 hydroxides. *J. Colloid Interface Sci.* **215**, 23-27.

784 Lec T. and Sadlik J. K. (2007) Contribution to the data on copper concentration in blood
785 and urine in patients with Wilson's disease and in normal subjects. *Biol. Trace Elem.*
786 *Res.* 118, 16-20.

787 Lee C. T., Yang W. T. and Parr R. G. (1988) Development of the colle-salvetti
788 correlation-energy formula into a functional of the electron-density. *Phys. Rev. B* **37**,
789 785-789.

790 Li W. Q., Jackson S. E., Pearson N. J., Alard O. and Chappell B. W. (2009) The Cu
791 isotopic signature of granites from the Lachlan Fold Belt, SE Australia. *Chem. Geol.*
792 **258**, 38-49.

793 Lippard S. J. and Berg J. M. (1994) *Principles of Bioinorganic Chemistry*, University
794 Science Books, Mill Valley.

- 795 Little S. H., Vance D., Sherman D. M. and Hein J.R. (2010) *Geochim. Cosmochim. Acta*
796 **74**, A608.
- 797 Liu X., Lu X., Meijer E. J. and Wang R. (2010) Hydration mechanisms of Cu²⁺: tetra-,
798 penta- or hexa-coordinated? *Phys. Chem. Chem. Phys.* **12**, 10801-10804.
- 799 Macleod, G., Mcneown, C., Hall, A. J., Russel, M. J. (1994) Hydrothermal and oceanic
800 pH conditions of possible relevance to the origin of life. *Origin Life Evol. Biosphere*
801 **24**, 19-41.
- 802 Magini, M. (1979) Solute structuring in aqueous iron(III) sulphate solutions. Evidence
803 for the formation of iron(III)-sulphate complexes. *J. Chem. Phys.* **70**, 317-324.
- 804 Magini M. (1982) Coordination of copper(II). Evidence of the Jahn-Teller effect
805 inaqueous perchlorate solutions. *Inorg. Chem.* **21**, 1535-1538.
- 806 Maréchal C. N., Telouk P. and Albarède F. (1999) Precise analysis of copper and zinc
807 isotopic compositions by plasma-source mass spectrometry. *Chem. Geol.* **156**,
808 51-273.
- 809 Maréchal C. and Albarède F. (2002) Ion-exchange fractionation of copper and zinc
810 isotopes. *Geochim. Cosmochim. Acta* **66**, 1499-1509.
- 811 Marini G. W., Liedl K. R. and Rode B. M. (1999) Investigation of Cu²⁺ hydration and
812 the Jahn-Teller effect in solution by QM/MM Monte Carlo simulations. *J. Phys.*
813 *Chem. A* **103**, 11387-11393.
- 814 Margolls S. A and Davis T. P. (1988) Stabilization of ascorbic acid in human plasma,
815 and its liquid-chromatographic measurement. *Clin. Chem.* **34**, 2217-2223.
- 816 Massey L. K., Liebman, M., Kynast-Gales S. A. (2005) Ascorbate increases human
817 oxaluria and kidney stone risk. *J. Nutrition* **135**, 1673-1677.

818 Mathur R., Ruiz J., Titley S., Liermann L., Buss H. and Brantley S. (2005) Cu isotopic
819 fractionation in the supergene environment with and without bacteria. *Geochim.*
820 *Cosmochim. Acta* **69**, 5233-5246.

821 Mathur R. Jin L., Prush V., Paul J., Ebersole C., Fornadel A., Williams J. Z. and
822 Brantley S. (2012) Cu isotopes and concentrations during weathering of black shale
823 of the Marcellus Formation, Huntingdon County, Pennsylvania (USA). *Chem. Geol.*
824 **304-305**, 175-184.

825 Matin M. D. A., Nomura M., Fujii Y. and Chen J. (1998) Isotope effects of copper in
826 ligand-exchange system and electron-exchange system observed by ion-exchange
827 displacement chromatography. *Sep. Sci. Technol.* **33**, 1075-1087.

828 Moffett J. W. (1995) Temporal and spatial variability of copper complexation by strong
829 chelators in the Sargasso Sea. *Deep Sea Res I* **42**, 1273-1295.

830 Moffett J. W. and Brand L. E. (1996) The production of strong, extracellular Cu
831 chelators by marine cyanobacteria in response to Cu stress. *Limnol. Oceanogr.* **41**,
832 388-395.

833 Morel F. M. M. and Hering J. G. (1993) *Principles and Applications of Aquatic*
834 *Chemistry*, John Wiley, New York.

835 Moynier F., Koeberl C., Beck P., Jourdan F. and Telouk P. (2010) Isotopic fractionation
836 of Cu in tektites. *Geochim. Cosmochim. Acta* **74**, 799-807.

837 Musinu A., Paschina G., Piccaluga G. and Magini M. (1983) Coordination of copper(II)
838 in aqueous CuSO₄ solution. *Inorg. Chem.* **22**, 1184-1187.

839 Nakamura E., Okubo K. and Namiki H. (1982) Butanol extraction of copper-zincon
840 complex with dibenzo-18-crown-6. *Bunseki Kagaku* **31**, 602-604.

841 Navarette J.U., Borrok D.M., Viveros M. and Ellzey J.T. (2011) Copper isotope
842 fractionation during surface adsorption and intracellular incorporation by bacteria.
843 *Geochim. Cosmochim. Acta* **75**, 784-799.

844 Neilson G. W. (1982) Cu²⁺ coordination in aqueous solution. *J. Phys. C: Solid State*
845 *Phys.* **15**, L233-L237.

846 Nishizawa K., Ishino S., Watanabe H. and Shinagawa M. (1984) Lithium isotope
847 separation by liquid-liquid extraction using benzo-15-crown-5. *J. Nucl. Sci. Technol.*
848 **21**, 694–701.

849 Nomura M., Higuchi N. and Fujii Y. (1996) Mass dependence of uranium isotope
850 effects in the U(IV)-U(VI) exchange reaction. *J. Am. Chem. Soc.* **118**, 9127-9130.

851 Nomura M. and Yamaguchi T. (1988) Concentration dependence of extended x-ray
852 absorption fine structure and x-ray absorption near-edge structure of copper(II)
853 perchlorate aqueous solution: comparison of solute structure in liquid and glassy
854 states. *J. Phys. Chem.* **92**, 6157-6160.

855 Ohtaki H and Maeda M. (1974) An x-ray diffraction study of the structure of hydrated
856 copper(II) ion in a copper(II) perchlorate solution. *Bull. Chem. Soc. Jpn.* **47**,
857 2197-2199.

858 Okan S. E. and Salmon P. S. (1995) The Jahn-Teller effect in solutions of flexible
859 molecules: a neutron diffraction study on the structure of a Cu²⁺ solution in ethylene
860 glycol. *Mol. Phys.* **85**, 981-998.

861 Pasquarello A., Petri I., Salmon P. S., Parisel O., Car R., Toth E., Powell D. H., Fischer
862 H. E, Helm L. and Merbach A. E. (2001) First solvation shell of the Cu(II) aqua ion:
863 evidence for fivefold coordination. *Science* **291**, 856-859.

864 Persson I., Persson P., Sandström M. and Ullström A. -S. (2002) Structure of
865 Jahn-Teller distorted solvated copper(II) ions in solution, and in solids with
866 apparently regular octahedral coordination geometry. *J. Chem. Soc., Dalton Trans.*
867 1256-1265.

868 Pokrovsky O. S., Viers J., Emnova E. E., Kompantseva E. I. and Freydier R. (2008)
869 Copper isotope fractionation during its interaction with soil and aquatic
870 microorganisms and metal oxy(hyd)oxides: Possible structural control. *Geochim.*
871 *Cosmochim. Acta* **72**, 1742-1757.

872 Pokrovsky O. S., Pokrovski G. S., Shirokova L. S., Gonzalez A. G., Emnova E. E. and
873 Feurtet-Mazel A. (2012) Chemical and structural status of copper associated with
874 oxygenic and anoxygenic phototrophs and heterotrophs: possible evolutionary
875 consequences. *Geobiol.* **10**, 130-149.

876 Pons M. L., Quitté G., Fujii T., Rosing M. T., Reynard B., Moynier F., Douchet C. and
877 and Albarède F. (2011) Early Archean serpentine mud volcanoes at Isua, Greenland,
878 as a niche for early life. *Proc. Natl. Acad. Sci. USA* **108** 17639-17643.

879 Pourbaix, M. (1974) *Atlas of electrochemical equilibria in aqueous solutions*. NACE,
880 Houston.

881 Rode B. M. and Islam S. M. (1992) Structure of aqueous copper chloride solutions:
882 results from Monte Carlo simulations at various concentrations. *J. Chem. Soc.,*
883 *Faraday Trans.* **88**, 417-422.

884 Roos B. O., Lindh R., Malmqvist P. -Å., Veryazov V. and Widmark P. -O. (2005) New
885 relativistic ANO basis sets for transition metal atoms. *J. Phys. Chem. A* **109**,
886 6575-6579.

887 Rustad J. R., Casey W. H., Yin Q. Z., Bylaska E. J., Felmy A. R., Bogatko S. A.,
888 Jackson V. E. and Dixon D. A. (2010) Isotopic fractionation of $\text{Mg}^{2+}(\text{aq})$, $\text{Ca}^{2+}(\text{aq})$,
889 and $\text{Fe}^{2+}(\text{aq})$ with carbonate minerals. *Geochim. Cosmochim. Acta* **74**, 6301-6323.

890 Salmon P. S. Neilson G. W. and Enderby J. E. (1988) The structure of Cu^{2+} aqueous
891 solutions. *J. Phys. C: Solid State Phys.* 21 1335-1349.

892 Schauble E. A. (2007) Role of nuclear volume in driving equilibrium stable isotope
893 fractionation of mercury, thallium, and other very heavy elements, *Geochim.*
894 *Cosmochim. Acta* **71**, 2170-2189.

895 Schwenk C. F. and Rode B. M. (2003a) New insights into the Jahn-Teller effect through
896 ab initio quantum-mechanical/molecular-mechanical molecular dynamics simulations
897 of Cu^{II} in water. *Chem. Phys. Chem.* **4**, 931-943.

898 Schwenk C. F. and Rode B. M. (2003b) Extended ab initio quantum
899 mechanical/molecular mechanical molecular dynamics simulations of hydrated Cu^{2+} .
900 *J. Chem. Phys.* **119**, 9523-9531.

901 Sherman D. M. (2001) Quantum chemistry and classical simulations of metal
902 complexes in aqueous solutions. *Rev. Mineral. Geochem.* **42**, 273-317.

903 Sham T. K., Hastings J. B. and Perlman M. L. (1981) Application of the EXAFS
904 method to Jhan-Teller ions: static and dynamic behavior of $\text{Cu}(\text{H}_2\text{O})_6^{2+}$ and
905 $\text{Cr}(\text{H}_2\text{O})_6^{2+}$ in aqueous solution. *Chem. Phys. Lett.* **83**, 391-396.

906 Shields W. R., Murphy T. J. and Garner E. L. (1964) Absolute isotopic abundance ratio
907 and the atomic weight of a reference sample of copper. *J. Res. NBS* 68A, 589-592.

908 Shields W. R., Goldich S. S., Garner E. L. and Murphy, T. J. (1965) Natural variations
909 in the abundance ratio and the atomic weight of copper. *J Geophys Res*, 7, 479-491.

910 Smith, R. M., Martell, A. E. (1989) *Critical stability constants*, vol. 6, 2nd Suppl.,
911 Plenum Press, New York.

912 Solomon E. I., Sundaram U. M and Machonkin T. E. (1996) Multicopper oxidases and
913 oxygenases. *Chem. Rev.* **96**, 2563-2605.

914 Tajiri Y. and Wakita H. (1986) An EXAFS investigation of the coordination structure of
915 copper(II) ions in aqueous $\text{Cu}(\text{ClO}_4)_2$ and methanolic CuCl_2 solutions. *Bull. Chem.*
916 *Soc. Jpn.* 59, 2285-2291.

917 Tanimizu M., Takahashi Y. and Nomura M. (2007) Spectroscopic study on the anion
918 exchange behavior of Cu chloro-complexes in HCl solutions and its implication to Cu
919 isotopic fractionation. *Geochem. J.* **41**, 291-295.

920 Texler N. R., Holdway S., Neilson G. W. and Rode B. M. (1998) Monte Carlo
921 simulations and neutron diffraction studies of the peptide forming system 0.5 mol
922 kg^{-1} CuCl_2 -5mol kg^{-1} NaCl - H_2O at 293 and 353 K. *J. Chem. Soc., Faraday Trans.*
923 **94**, 59-65.

924 Tsuchiya T., Abe M., Nakajima T. and Hirao K. (2001) Accurate relativistic Gaussian
925 basis sets for H through Lr determined by atomic self-consistent field calculations
926 with the third-order Douglas-Kroll approximation. *J. Chem. Phys.* **115**, 4463-4472.

927 van Duin A. C. T., Bryantsev V. S., Diallo M. S., Goddard W. A., Rahaman O., Doren
928 D. J., Raymond D. and Hermansson K. (2010) Development and validation of a
929 ReaxFF reactive force field for Cu cation/water interactions and copper metal/metal
930 oxide/metal hydroxide condensed phases. *J. Phys. Chem. A* **114**, 9507-9514.

931 van Rossum J. P. and Scharhart D. H. J. (1991) Oxidation-reduction (redox)
932 potentiometry in blood in geriatric conditions: a pilot study. *Exper. Gerontol.* **26**,
933 37-43.

934 Vance D., Archer C., Bermin J., Perkins J., Statham P. J., Lohan M. C., Ellwood M. J.
935 and Mills R. A. (2008) The copper isotope geochemistry of rivers and the oceans.
936 *Earth Planet. Sci. Lett.* **274**, 204-213.

937 Walker E. C., Cuttitta F. and Senfle F. E. (1958) Some natural variations in the relative
938 abundance of copper isotopes. *Geochim. Cosmochim. Acta* **15**, 183-194.

939 Weinstein C., Moynier F., Wang K., Paniello R., Foriel J. Catalano J. and Pichat S.
940 (2011) Isotopic fractionation of Cu in plants. *Chem. Geol.* **286**, 266-271.

941 Yoshio M., Ugamura M., Noguchi H. and Nagamatsu M. (1980) Applications of crown
942 ether in chemical analysis extraction of copper(II)-zincon chelate anion with crown
943 ether complex. *Anal. Lett.* **13**, 1431-1439.

944 Zhu X. K., O’Nions R. K., Guo Y., Belshaw N. S. and Rickard D. (2000) Determination
945 of Cu-isotope variation by plasma-source mass spectrometry: implications for use as
946 geochemical tracers. *Chem. Geol.* **163**, 139-149.

947 Zhu X. K., Guo Y., Williams R. J. P., O’Nions R. K., Matthews A., Belshaw N. S.,
948 Canters G. W., de Waal E. C., Weser U., Burgess B. K. and Salvato B. (2002) Mass
949 fractionation processes of transition metal isotopes. *Earth Planet. Sci. Lett.* **200**,
950 47-62.

951 Zirino A. and Yamamoto S (1972) A pH-dependent model for the chemical speciation
952 of copper zinc cadmium, and lead in seawater. *Limnol. Oceanogr.* **17**, 661-671.

953

954

955
956
957
958
959
960
961
962
963
964
965
966

967 Table 1 Isotopic fractionation of Cu(II) during
968 exchange experiments between HCl medium and a
969 macrocyclic complex.

[HCl] (M)	<i>D</i>	$\Delta^{65}\text{Cu}^a$ (‰)
1	1.3×10^{-4}	-1.06
2	1.8×10^{-3}	-0.84
3	2.4×10^{-2}	-0.77
4	1.5×10^{-1}	-0.65
5	4.6×10^{-1}	-0.61
6	9.8×10^{-1}	-0.39

970 ^a Errors are $\pm 0.10\%$ for 2σ .

971

972

973

974

975

976

977

978

979

980

Table 2 Nuclear field shift effect of Cu isotopes and isotopologues at 298 K.

Valence	Species	Total energy (a.u.)		ΔE (a.u.) (10^{-5})	Nuclear Field shift effect (‰)
		^{63}Cu	^{65}Cu		
Cu(0)	Cu^0	-1653.451898480	-1653.451827445	7.1035	-0.014
Cu(I)	Cu^+	-1653.210583752	-1653.210512731	7.1021	0.001
	CuCl	-2114.481787065	-2114.481716036	7.1029	-0.007
	CuH_2O^+	-1729.354508434	-1729.354437410	7.1024	-0.002
	CuOH	-1728.963440770	-1728.963369739	7.1031	-0.010
Cu(II)	Cu^{2+}	-1652.578696630	-1652.578625608	7.1022	0
	CuCl^+	-2114.155110496	-2114.155039471	7.1025	-0.003
	$\text{CuH}_2\text{O}^{2+}$	-1728.798913392	-1728.798842366	7.1026	-0.004
	CuOH^+	-1728.656622258	-1728.656551226	7.1032	-0.011
	CuO	-1728.336259331	-1728.336188299	7.1032	-0.011

981

^a The nuclear field shift effect was calculated by $(\delta E_{\text{reference}} - \delta E_{\text{species}})/kT$ at $T = 298\text{K}$.

982

The root-mean-square charge radii $\langle r^2 \rangle^{1/2}$ reported for ^{63}Cu (3.8823×10^{-15} m) and ^{65}Cu

983

(3.9022×10^{-15} m) (Angeli, 2004) were used. Cu^{2+} was set as the reference. Energy of

984

photons of 1 a.u. is equal to 4.3597×10^{-18} J.

985

986

987

988

989

990

991

992

993 Table 3 Bond distances determined for $\text{Cu}(\text{H}_2\text{O})_6^{2+}$.

Cu-O _{ax} (Å)	Cu-O _{eq} (Å)	Method ^a	Reference
2.30	2.02-2.03	MO	This study
2.25	2.06	MO	Beagley et al., 1989
2.25	2.05	MO	Åkesson et al., 1992
2.25	2.06-2.07	MO	Breza et al., 1997
2.23-2.26	2.033	MO	Bryantsev et al., 2008
2.46-2.58	1.97-2.09	MD	Liu et al., 2010
2.27	1.94	QM	van Duin et al., 2010
2.24	2.07	QM/MM MC	Marini et al., 1999
2.2-2.3	1.99-2.07	QM/MM MD	Schwenk and Rode, 2003a,b
2.60	1.955	EXAFS	Sham et al., 1981
2.28	2.00	EXAFS	Tajiri and Wakita, 1986
2.3	1.96	EXAFS	Nomura and Yamaguchi, 1988
2.29	1.99	EXAFS	Beagley et al., 1989
2.375-2.413	1.969-1.971	EXAFS	Fulton et al., 2000a,b
2.30	1.955	EXAFS	Persson et al., 2002
2.56	1.99	EXAFS+XANES	Benfatto et al., 2002
2.36	1.96	EXAFS+XANES	Chaboy et al., 2006
2.32	1.96	XANAS	Garcia et al., 1989
≥2.21	1.96	ND	Salmon et al., 1988
2.45	1.95	ND	Okan and Salmon, 1995
2.43	1.94	XRD	Ohtaki and Maeda, 1974
2.339	1.976	XRD	Magini, 1982

994 ^a MO (molecular orbital), EXAFS(extended x-ray absorption fine structure), MD
 995 (molecular dynamics), ND (neutron diffraction), QM(quantum mechanics), MM
 996 (molecular mechanics), MC (Monte Carlo), XANES (x-ray absorption near-edge
 997 structure), and XRD(x-ray diffraction).

998

999

1000

1001

1002

1003

1004
 1005
 1006
 1007
 1008
 1009
 1010
 1011
 1012
 1013
 1014
 1015
 1016

Table 4 Bond distances determined for $\text{Cu}(\text{H}_2\text{O})_5^{2+}$.

Cu-O _{long} (Å)	Cu-O _{short} (Å)	Method ^a	References
2.20	1.99-2.02	MO	This study
2.181	2.011	MO	Bryantsev et al., 2008
2.45	2.00	CPMD	Amira et al., 2005
2.22	2.04-2.07	CPMD	de Almeida et al., 2009
2.31	2.03-2.09	MD	Liu et al., 2010
2.34	1.963	EXAFS	Persson et al., 2002
2.39	1.97	EXAFS+XANES	Benfatto et al., 2002
2.36	1.96	EXAFS+XANES	Chaboy et al., 2006
–	1.96	ND	Pasquarello et al., 2001

1017 ^a CPMD (Car-Parrinello MD)

1018
 1019
 1020
 1021
 1022
 1023
 1024
 1025
 1026
 1027
 1028
 1029
 1030
 1031
 1032
 1033
 1034

1035
 1036
 1037
 1038
 1039
 1040
 1041
 1042
 1043
 1044
 1045
 1046
 1047
 1048
 1049

Table 5 Logarithm of the reduced partition function, $\ln \beta$, for the pair ^{65}Cu - ^{63}Cu .
 Hydrated Cu(II) ions and chlorides.

Species	Temperature (K)					
	273	298	323	373	473	573
$\text{Cu}(\text{H}_2\text{O})_5^{2+}$	5.355	4.546	3.905	2.968	1.876	1.290
$\text{Cu}(\text{H}_2\text{O})_6^{2+}$	5.053	4.288	3.682	2.798	1.767	1.215
$\text{CuCl}(\text{H}_2\text{O})_4^+$	4.906	4.161	3.572	2.712	1.711	1.176
$\text{CuCl}_2(\text{H}_2\text{O})_3$	4.709	3.988	3.420	2.592	1.633	1.120
$\text{CuCl}_2(\text{H}_2\text{O})_4$	4.397	3.724	3.193	2.421	1.525	1.046
$\text{CuCl}_3\text{H}_2\text{O}^-$	3.530	2.985	2.556	1.933	1.214	0.832

1052
 1053
 1054
 1055
 1056
 1057
 1058
 1059
 1060
 1061
 1062
 1063
 1064
 1065
 1066
 1067

1068
 1069
 1070
 1071
 1072
 1073
 1074
 1075

Table 6 Bond distances determined for $\text{CuCl}_m(\text{H}_2\text{O})_n^{2-m}$.

Possible species	<i>m</i>	<i>n</i>	Cu-Cl ^a (Å)	Cu-O ^a (Å)	Method	References
$\text{CuCl}(\text{H}_2\text{O})_4^+$	1	4	2.20	2.04-2.06(3) 2.35(1)	MO	This study
$\text{CuCl}(\text{H}_2\text{O})_4^+$	1 ^b	4	2.29 ^b	1.968(3) 2.27(1)	EXAFS	D'Angelo et al., 1997
$\text{CuCl}(\text{H}_2\text{O})_5^+$	1.1	5.2	2.55	2.00	MC	Rode and Islam, 1992
$\text{CuCl}_2(\text{H}_2\text{O})_3$	2	3	2.25	2.07-2.08(2) 2.35(1)	MO	This study
$\text{CuCl}_2(\text{H}_2\text{O})_3$	2.0	3.3	3.1	1.96	ND	Ansell et al, 1995
$\text{CuCl}_2(\text{H}_2\text{O})_4$	2	4	2.27	2.11(2) 2.43(2)	MO	This study
$\text{CuCl}_2(\text{H}_2\text{O})_4$	2	4	2.22	2.01(2) 2.28(2)	EXAFS	Tajiri and Wakita, 1986
$\text{CuCl}_2(\text{H}_2\text{O})_4$	2.8	4.3	2.56	2.05(2) 2.5(2)	ND	Neilson, 1982
$\text{CuCl}_3\text{H}_2\text{O}^-$	3	1	2.22(1) 2.28(2)	2.28	MO	This study
$\text{CuCl}_3\text{H}_2\text{O}^-$	2.1	1	2.28	1.95	EXAFS	Collings et al., 2000
$\text{CuCl}_3(\text{H}_2\text{O})_3^-$	3.3	2.7	2.43	1.90-1.95	XRD	Bell et al., 1973
CuCl_4^{2-}	3.8	0	2.24	–	EXAFS	Tanimizu et al., 2007
$\text{CuCl}_4(\text{H}_2\text{O})_2^{2-}$	3.8	1.9	2.23	2.18	EXAFS	Tanimizu et al., 2007
$\text{CuCl}_4(\text{H}_2\text{O})_2^{2-}$	4.2	2.3	2.56	2.05	ND	Neilson, 1982
$\text{CuCl}_4(\text{H}_2\text{O})_2^{2-}$	3.6	2.4	2.43	1.90-1.95	XRD	Bell et al., 1973

1076
 1077
 1078
 1079
 1080
 1081
 1082
 1083

^a Number of bonds is shown in parentheses.

^b An additional Cu-Cl bond distance of 2.85 Å reported may be too long to treat as chemical bonding.

1084
 1085
 1086
 1087
 1088
 1089
 1090
 1091
 1092
 1093
 1094
 1095

1096 Table 7 Logarithm of the reduced partition function, $\ln \beta$, for the pair ^{65}Cu - ^{63}Cu .
 1097 Cu(II) hydroxides, carbonates, sulfate, and sulfides.

Species	Temperature (K)					
	273	298	323	373	473	573
$\text{CuOH}(\text{H}_2\text{O})_4^+$	5.307	4.517	3.889	2.967	1.883	1.298
$\text{Cu}(\text{OH})_2(\text{H}_2\text{O})_3$	5.814	4.966	4.288	3.286	2.098	1.451
$\text{CuCO}_3(\text{H}_2\text{O})_2$	5.091	4.323	3.715	2.825	1.787	1.230
$\text{Cu}(\text{CO}_3)_2^{2-}$	6.176	5.239	4.498	3.416	2.158	1.483
$\text{CuHCO}_3(\text{OH})_2^-$	5.951	5.075	4.376	3.346	2.130	1.471
$\text{CuSO}_4(\text{H}_2\text{O})_4$	6.041	5.144	4.430	3.381	2.148	1.481
$\text{CuHS}(\text{H}_2\text{O})_4^+$	4.002	3.386	2.900	2.194	1.377	0.942
$\text{Cu}(\text{HS})_2(\text{H}_2\text{O})_3$	3.855	3.264	2.797	2.119	1.333	0.914

1098
 1099
 1100
 1101
 1102
 1103
 1104
 1105
 1106

1107

1108

1109

1110

1111

1112

1113

1114

1115 Table 8 Logarithm of the reduced partition function, $\ln \beta$, for the pair ^{65}Cu - ^{63}Cu .

1116 Hydrated Cu(I) ion, Cu(II) ascorbates, and Cu(II) oxalate.

Species	Temperature (K)					
	273	298	323	373	473	573
$\text{Cu}(\text{H}_2\text{O})_2^+$, Cu(I)	3.368	2.867	2.468	1.882	1.193	0.822
$\text{CuH}(\text{L-asorbate})(\text{H}_2\text{O})_4^+$	3.924	3.324	2.850	2.161	1.362	0.935
$\text{CuH}(\text{D-asorbate})(\text{H}_2\text{O})_4^+$	3.989	3.380	2.899	2.199	1.386	0.951
$\text{CuC}_2\text{O}_4(\text{H}_2\text{O})_2$	6.236	5.302	4.561	3.474	2.202	1.516

1117

1118

1119

1120

1121

1122 **Figure captions**

1123 **Figure 1 Mole fractions of Cu species and isotope fractionation of Cu in HCl**
1124 **solutions.** a) Distribution of Cu chlorides. The mole fractions were calculated from the
1125 stability constants of Brugger (2001). b) Isotope fractionation is shown as $\Delta^{65}\text{Cu} =$
1126 $\delta^{65}\text{Cu}_{\text{org}} - \delta^{65}\text{Cu}_{\text{aq}}$ upon extraction of Cu by dicyclohexano-18-crown-6 (DC18C6) from
1127 the aqueous solution. The solid curves represent our estimates from the $\ln \beta$ values (298
1128 K) of fivefold-coordinated $\text{Cu}(\text{H}_2\text{O})_5^{2+}$, $\text{CuCl}(\text{H}_2\text{O})_4^{2+}$, and $\text{CuCl}_2(\text{H}_2\text{O})_3$, and
1129 $\text{CuCl}_3\text{H}_2\text{O}^-$ (Table 5), $\ln \beta_{\text{CuLCl}_2}$ (3.35‰), and D . The dotted curves represent the effect
1130 of $\pm 0.05\text{‰}$ errors on $\ln \beta_{\text{CuLCl}_2}$.

1131 **Figure 2. Molecular structures of hydrated Cu^+ , Cu^{2+} , and aqueous Cu(II) species.**
1132 The structures are drawn using GaussView5 (Gaussian Inc.) (Dannington et al., 2009).
1133 Symbol keys: Cu (vermilion), Cl (green), S (yellow), O (red), C (gray), and H (white).

1134 **Figure 3. Temperature dependence of $\ln \beta$.** The $\ln \beta$ values of hydrated Cu^{2+} and
1135 Cu(II) chlorides (see Table 5) are shown as linear functions of T^2 .

1136 **Figure 4. Mole fractions of Cu(II) species and Cu isotopic variations as functions of**
1137 **pH at 298 K.** a) Mole fractions of Cu species, b) Species $\delta^{65}\text{Cu}$ relative to the bulk
1138 solution. Literature values of formation constants at ionic strength $I = 0.70$ M (Powell et
1139 al., 2007) were used for the calculations. $\Sigma[\text{Cu(II)}]$ was set to 10^{-9} M and it was
1140 assumed that the system was in equilibrium with air having a CO_2 fugacity of $10^{-3.5}$ bar
1141 ($1 \text{ bar} = 10^5 \text{ Pa}$) (Powell et al., 2007). We further assumed $\log K[\text{CO}_2(\text{g}) = \text{CO}_2(\text{aq})] =$
1142 -1.5 (Morel and Hering, 1993) and concentrations of $\text{Cl}^- = 0.55 \text{ mol kg}^{-1}$ and $\text{SO}_4^{2-} =$
1143 $0.029 \text{ mol kg}^{-1}$ (Macleod et al., 1994).

1144 **Figure 5. Temperature dependence of $\ln \beta$.** The $\ln \beta$ values of hydrated Cu(II)
1145 hydroxides, carbonates, sulfate, and sulfides (see Table 7) are shown as linear functions
1146 of T^2 .

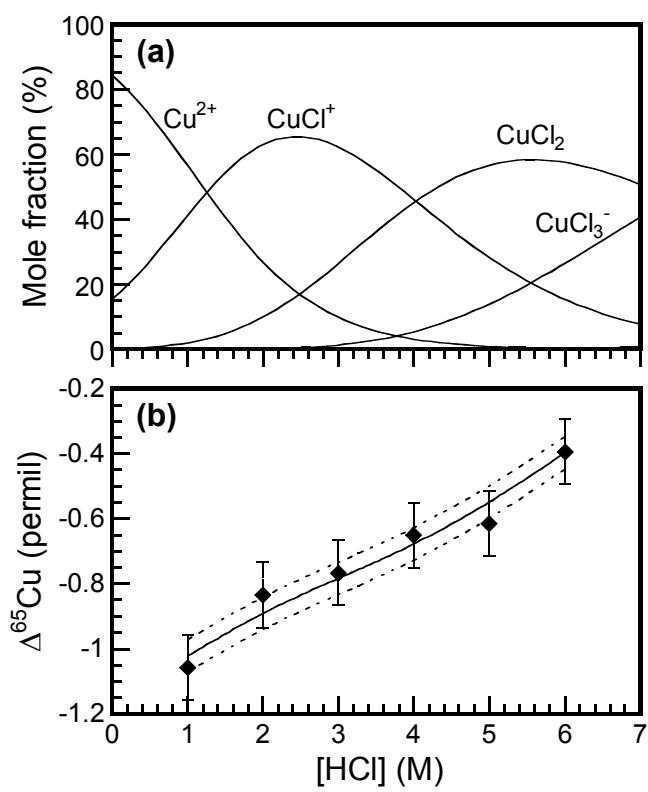
1147 **Figure 6. Mole fractions of Cu(I) and Cu(II) species and Cu isotopic variations as**
1148 **functions of Eh and extent of oxalate formation at 298 K.** pH and total Cu
1149 concentration were set to be 7.4 and 1 μM , respectively a) Mole fractions of Cu species
1150 as functions of Eh. Concentrations of ascorbate and oxalate were set to 90 μM and 10
1151 μM , respectively. b) Mole fractions of Cu species as functions of proportion of oxalate
1152 formed. Eh was set to be 0.27 V. c) $\delta^{65}\text{Cu}$ relative to the bulk solution as functions of
1153 Eh. Conditions are identical to those of a, and d) $\delta^{65}\text{Cu}$ relative to the bulk solution as
1154 functions of extent of oxalate formation. Conditions are identical to those of b.

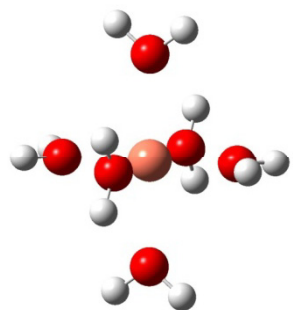
1155 **Figure 7. Temperature dependence of $\ln \beta$.** The $\ln \beta$ values of hydrated Cu^+ and
1156 Cu(II) oxalate and ascorbate (see Table 8) are shown as linear functions of T^2 . The $\ln \beta$
1157 values of pentaqua Cu^{2+} (see Table 5 and Fig. 3) are shown together.

1158

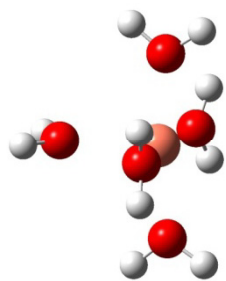
1159

1160

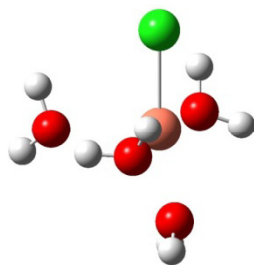




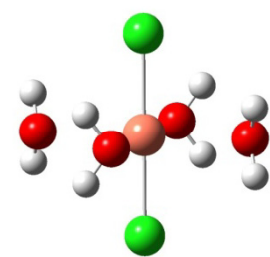
a) $\text{Cu}(\text{H}_2\text{O})_6^{2+}$



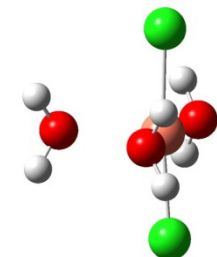
b) $\text{Cu}(\text{H}_2\text{O})_5^{2+}$



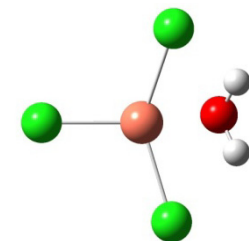
c) $\text{CuCl}(\text{H}_2\text{O})_4^+$



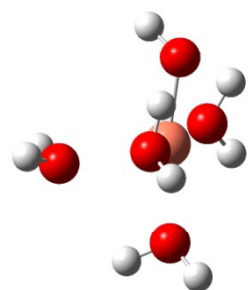
d) $\text{CuCl}_2(\text{H}_2\text{O})_4$



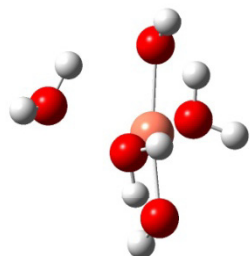
e) $\text{CuCl}_2(\text{H}_2\text{O})_3$



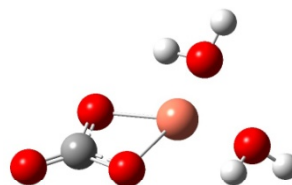
f) $\text{CuCl}_3\text{H}_2\text{O}^-$



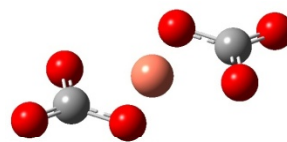
g) $\text{CuOH}(\text{H}_2\text{O})_4^-$



h) $\text{Cu}(\text{OH})_2(\text{H}_2\text{O})_3$



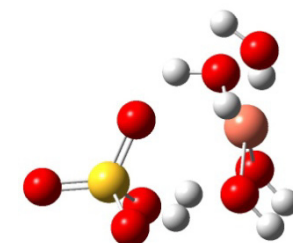
i) $\text{CuCO}_3(\text{H}_2\text{O})_2$



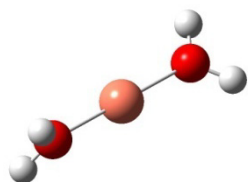
j) $\text{Cu}(\text{CO}_3)_2^{2-}$



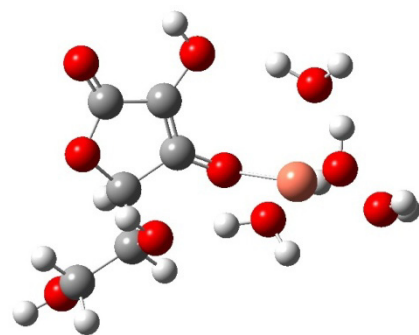
k) $\text{CuHCO}_3(\text{OH})_2^-$



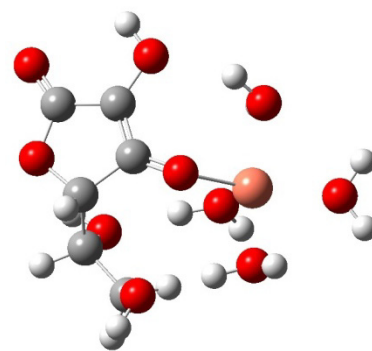
l) $\text{CuSO}_4(\text{H}_2\text{O})_4$



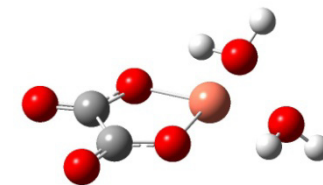
m) $\text{Cu}(\text{H}_2\text{O})_2^+$, Cu(I)



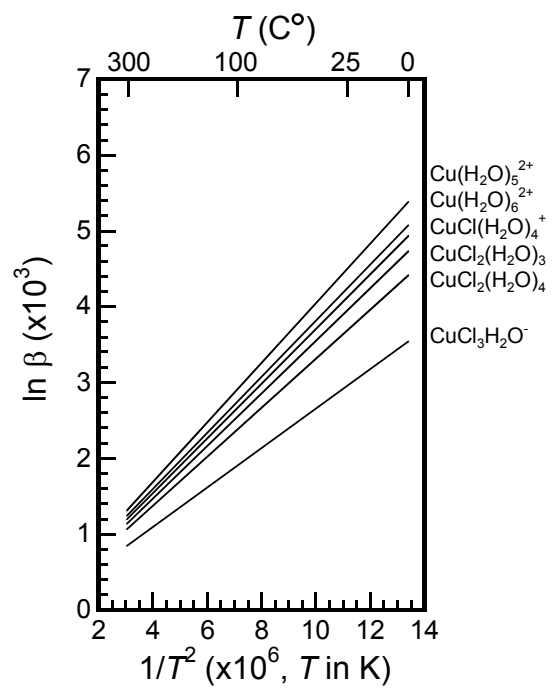
n) $\text{CuHA}(\text{H}_2\text{O})_4^+$
(A: L-ascorbate)

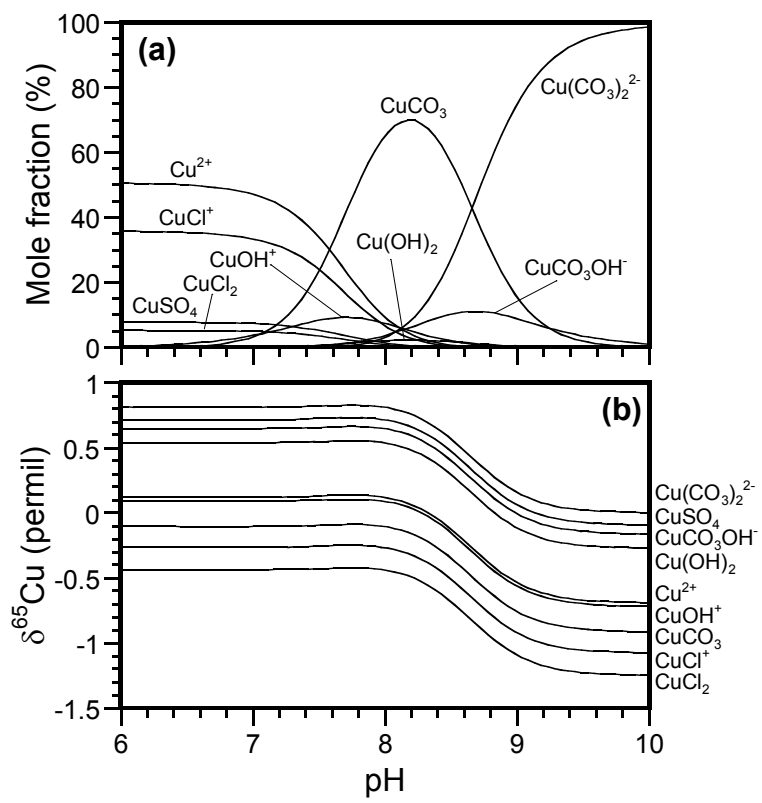


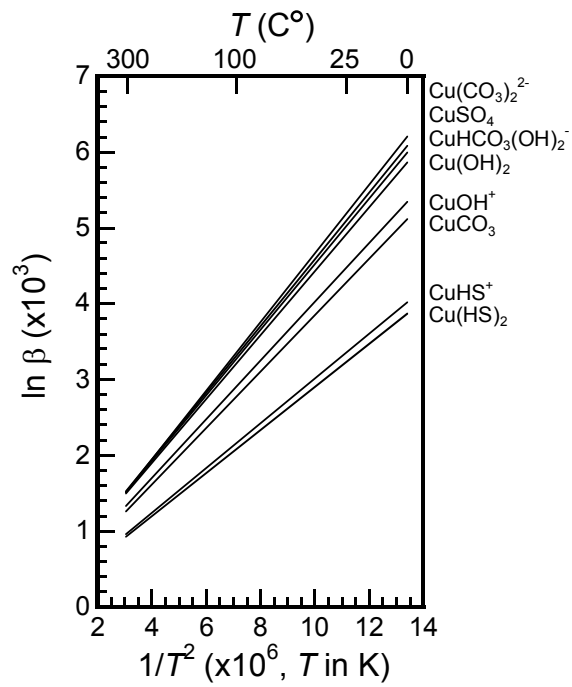
o) $\text{CuHA}(\text{H}_2\text{O})_4^+$
(A: D-ascorbate)

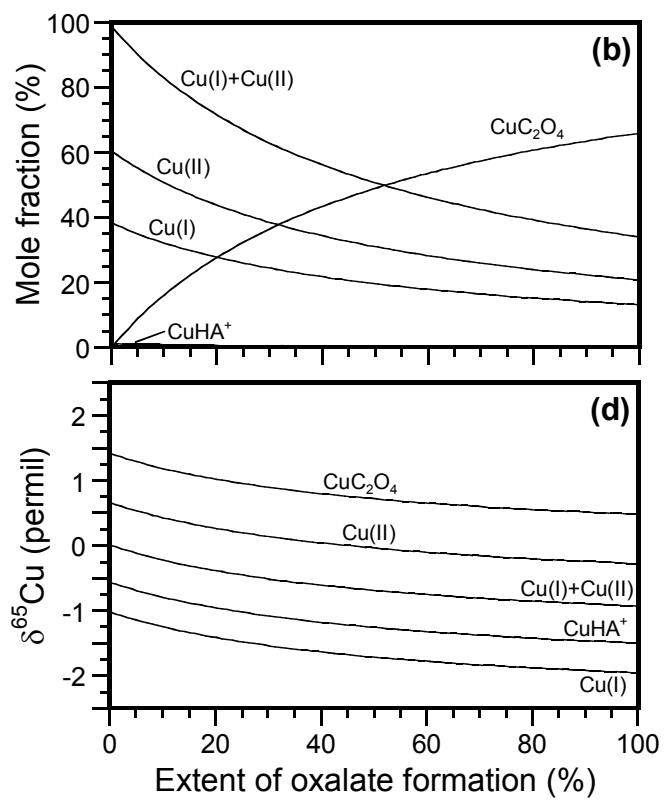
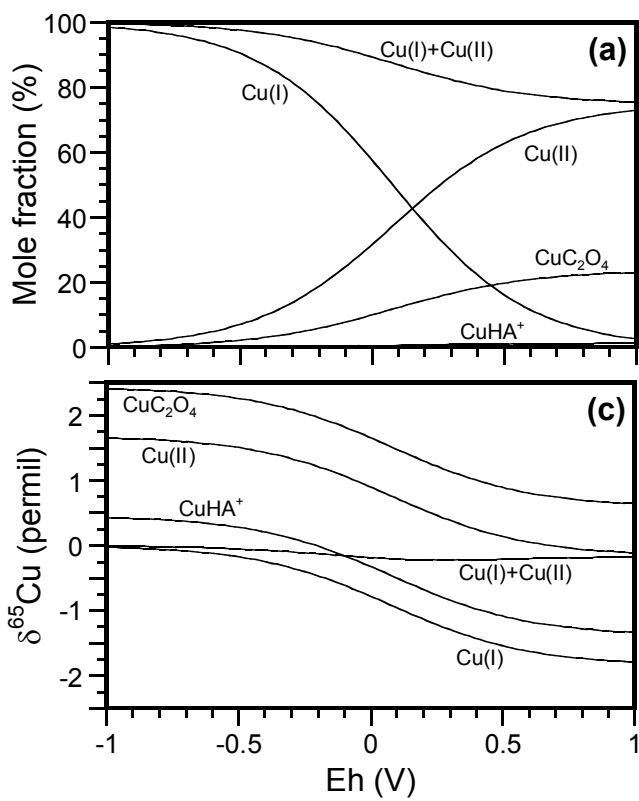


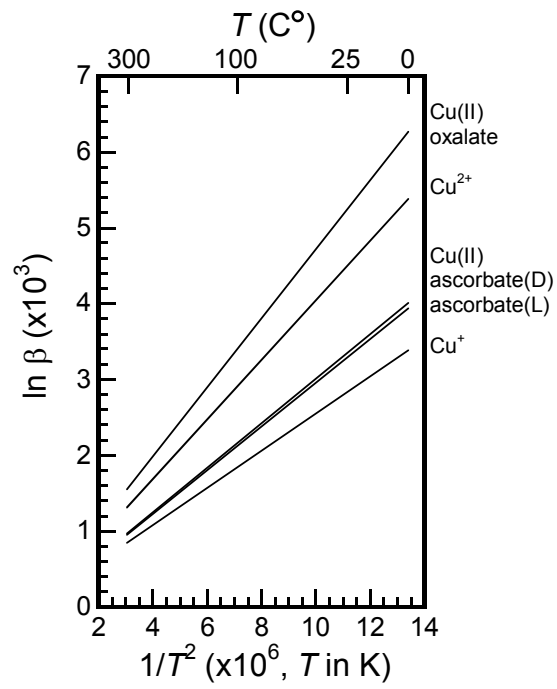
p) $\text{CuC}_2\text{O}_4(\text{H}_2\text{O})_2$











Supporting Information

Copper isotope fractionation between aqueous compounds relevant to low temperature geochemistry and biology

Toshiyuki Fujii^{1*}, Frédéric Moynier², Minori Abe³,
Keisuke Nemoto³, and Francis Albarède⁴

¹ Research Reactor Institute, Kyoto University, 2-1010 Asashiro Nishi, Kumatori, Sennan, Osaka 590-0494, Japan

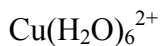
² Department of Earth and Planetary Sciences and McDonnell Center for Space Sciences, Washington University in St. Louis, Campus Box 1169, 1 Brookings Drive, Saint Louis, MO 63130-4862, USA

³ Department of Chemistry, Graduate School of Science and Engineering, Tokyo Metropolitan University, 1-1 Minami-Osawa, Hachioji-shi, Tokyo 192-0397, Japan

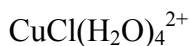
⁴ Ecole Normale Supérieure de Lyon, Université de Lyon 1, CNRS, 46, Allée d'Italie, 69364 Lyon Cedex 7, France

Table S1. Optimized structure Cartesian coordinates of hydrated Cu(I) and Cu(II) ions and Cu(II) complexes. (see Figure 2).

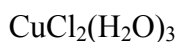
Cu(H ₂ O) ₅ ²⁺			
Element	X	Y	Z
Cu	0.000000	0.000000	0.180286
O	-0.000218	1.972347	0.416359
O	-2.015695	0.000003	0.367094
O	0.000218	-1.972347	0.416359
O	2.015695	-0.000003	0.367094
O	0.000000	0.000000	-2.017628
H	-0.788497	2.520100	0.544468
H	0.787668	2.520277	0.546113
H	-0.787668	-2.520277	0.546113
H	0.788497	-2.520100	0.544468
H	-2.541191	0.000171	1.181710
H	-2.620652	-0.000935	-0.390193
H	2.541191	-0.000171	1.181710
H	2.620652	0.000935	-0.390193
H	-0.000087	0.774145	-2.598417
H	0.000087	-0.774145	-2.598417



Element	X	Y	Z
Cu	0.000038	-0.000034	0.000063
O	-0.088873	2.019575	0.031113
O	-0.024969	-0.086591	2.300836
O	2.025399	0.080251	0.024068
O	0.088810	-2.019630	-0.031022
O	0.024925	0.086561	-2.300618
O	-2.025376	-0.080204	-0.023865
H	0.668784	2.613652	0.123299
H	-0.902057	2.538568	0.101414
H	0.902001	-2.538615	-0.101323
H	-0.668838	-2.613716	-0.123240
H	-0.067738	0.644710	2.931884
H	0.005459	-0.892336	2.834501
H	-0.005323	0.892306	-2.834292
H	0.067755	-0.644755	-2.931647
H	2.576945	0.077097	0.819263
H	2.591990	0.154602	-0.756953
H	-2.591929	-0.154550	0.757185
H	-2.576976	-0.076949	-0.819023



Element	X	Y	Z
Cu	-0.016654	0.212129	-0.176174
Cl	-0.368293	-1.902143	-0.655033
O	-0.263347	-0.047793	1.850095
O	2.209959	-0.237365	0.440996
O	-0.036021	2.218349	0.250375
O	-0.057535	0.711653	-2.157294
H	0.598254	-0.331813	2.193790
H	-0.889110	-0.757015	2.061119
H	0.438028	2.925105	-0.204498
H	-0.248494	2.513422	1.145250
H	3.038932	0.256513	0.412129
H	2.414530	-1.133283	0.138808
H	-0.785481	1.250808	-2.496952
H	-0.059913	-0.113878	-2.668013



Element	X	Y	Z
Cu	-0.053962	0.000888	-0.169852
Cl	0.052761	2.249760	-0.117204
Cl	0.050030	-2.247826	-0.115168
O	-0.166668	0.001703	1.905225
O	0.472730	-0.000037	-2.167140

O	-2.337733	0.004542	-0.702549
H	0.114046	0.787034	-2.597917
H	0.111330	-0.785773	-2.598069
H	0.267547	-0.788948	2.253624
H	0.269249	0.791416	2.253590
H	-2.746356	0.783330	-0.306552
H	-2.752723	-0.768865	-0.302717

 $\text{CuCl}_2(\text{H}_2\text{O})_4$

Element	X	Y	Z
Cu	0.000113	-0.000205	0.000036
Cl	0.001187	-2.268694	0.000102
Cl	-0.000962	2.268241	-0.000026
O	0.417498	0.000178	2.071588
O	2.327682	0.000039	-0.692256
O	-0.417251	-0.000257	-2.071517
O	-2.327453	-0.001831	0.692327
H	-2.708483	-0.776704	0.262520
H	-2.710171	0.772049	0.262246
H	0.031352	0.780962	-2.422591
H	0.032951	-0.780315	-2.423107
H	2.709142	-0.774664	-0.262522
H	2.709964	0.774089	-0.262095
H	-0.031968	0.780871	2.422726
H	-0.031827	-0.780407	2.423132

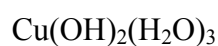
 $\text{CuCl}_3\text{H}_2\text{O}^-$

Element	X	Y	Z
Cu	0.009270	0.089718	-0.002037
Cl	2.197046	0.600440	0.407279
Cl	-0.053553	-0.775059	-2.050390
Cl	-2.075181	0.930696	0.398702
O	-0.031900	-0.399468	2.220232
H	-0.770277	0.213170	2.362199
H	0.792853	0.090825	2.362505

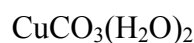
 $\text{CuOH}(\text{H}_2\text{O})_4^+$

Element	X	Y	Z
Cu	-0.022412	-0.011572	0.135042
O	2.055857	0.070828	-0.052489
O	-2.050422	0.169765	-0.181485
O	0.159947	1.789601	-0.261094
O	-0.205225	-2.061829	0.224458
O	0.053073	-0.361275	2.421138
H	2.051118	1.010485	-0.319345
H	2.660380	-0.414596	-0.627116
H	-2.204931	0.986925	-0.676734

H	-2.650954	-0.512055	-0.507452
H	-0.097467	2.412135	0.429233
H	-0.047966	-2.399730	1.116909
H	0.091646	-2.725054	-0.410229
H	0.872675	-0.124189	2.873930
H	-0.665321	-0.109440	3.015233



Element	X	Y	Z
Cu	-0.258245	-0.086613	-0.062472
O	-0.074679	-0.232907	1.820662
O	2.081764	0.067472	0.259624
O	-0.399476	2.106958	-0.460200
O	-0.677539	0.056454	-1.875154
O	-0.551081	-2.201797	0.273191
H	-0.175399	-0.497968	-2.477903
H	-1.413113	-2.553797	0.027322
H	-0.566410	-1.987168	1.228999
H	2.369866	0.976539	0.124900
H	1.738922	0.025664	1.174903
H	-1.195357	2.594308	-0.223017
H	-0.543869	1.724067	-1.363498
H	-0.468696	0.448284	2.370949

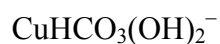


Element	X	Y	Z
Cu	0.248982	0.000870	-0.001777
O	1.470106	1.668045	-0.237640
O	1.470728	-1.665996	0.239991
O	-1.340955	1.081270	-0.128922
O	-1.338478	-1.082522	0.125223
O	-3.325503	-0.003074	-0.002008
C	-2.117328	-0.001419	-0.001917
H	2.092931	1.971316	0.432853
H	0.791443	2.353819	-0.329161
H	0.791117	-2.351065	0.329900
H	2.096954	-1.971245	-0.426543

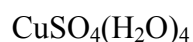


Element	X	Y	Z
Cu	0.000000	0.000000	0.000000
O	1.670093	1.094791	0.000000
O	1.670093	-1.094791	0.000000
O	-1.670093	1.094791	0.000000
O	-1.670093	-1.094791	0.000000
O	3.658669	0.000000	0.000000
O	-3.658669	0.000000	0.000000

C	2.413378	0.000000	0.000000
C	-2.413378	0.000000	0.000000



Element	X	Y	Z
Cu	0.328828	-0.274402	0.333280
O	-0.217938	0.652837	1.889544
O	2.152371	-0.434121	0.505155
O	-1.358315	-0.720389	-0.512057
O	-2.850925	-0.477652	-2.183668
O	-0.850477	0.562886	-2.262179
C	-1.778817	-0.270627	-1.625885
H	2.446380	-0.021985	1.321861
H	-1.181615	0.642755	1.857756
H	-1.280353	0.840660	-3.079424



Element	X	Y	Z
Cu	0.747523	-0.018631	0.075914
S	-2.464712	0.089386	0.319198
O	0.888308	1.472448	-1.374296
O	1.260468	-1.547098	-1.216183
O	-1.460921	0.074115	-0.784172
O	-3.860376	0.146652	-0.015297
O	-2.105782	1.314366	1.248990
O	-2.198978	-1.199463	1.194935
O	0.426005	1.463763	1.245656
O	0.334120	-1.521773	1.204522
H	0.822684	1.412610	2.120663
H	0.727408	-1.537786	2.082364
H	-1.070215	1.435319	1.324962
H	-1.181852	-1.395474	1.269655
H	-0.031570	1.461652	-1.687718
H	0.699514	-1.631741	-1.997308
H	0.934346	2.226004	-0.763219
H	0.994031	-2.244346	-0.588664



Element	X	Y	Z
Cu	0.005656	0.054181	0.049629
S	0.046759	2.225860	-0.652513
O	2.066189	0.034639	0.017085
O	-2.046642	0.067176	-0.000969
O	-0.098475	-2.084607	0.119384
O	-0.014729	-0.342819	2.333240
H	2.342733	0.886375	-0.359080
H	2.619756	-0.660348	-0.362321

H	-2.350685	0.888640	-0.417416
H	-2.561894	-0.668691	-0.356925
H	0.013829	2.775894	0.581471
H	-0.038801	-2.444466	1.013933
H	0.055219	-2.798994	-0.509691
H	0.752827	-0.111541	2.871191
H	-0.791745	-0.101300	2.852979

$\text{Cu}(\text{HS})_2(\text{H}_2\text{O})_3$

Element	X	Y	Z
Cu	-0.314974	-0.153083	0.141975
S	-0.177791	-0.026204	2.425827
S	-0.977088	-0.352010	-2.086603
O	2.022133	0.047647	0.018214
O	-0.359897	2.013095	-0.277947
O	-0.584294	-2.264904	0.309083
H	0.260936	-0.547023	-2.586321
H	-1.025393	-2.457587	-0.533692
H	-1.180639	-2.509597	1.028124
H	2.206699	0.965967	-0.211249
H	2.078845	0.012600	0.986178
H	-1.007256	2.546627	0.198468
H	-0.707717	1.864863	-1.179080
H	-0.366876	1.299105	2.585329

$\text{Cu}(\text{H}_2\text{O})_2^+, \text{Cu}(\text{I})$

Element	X	Y	Z
Cu	0.000000	0.000000	0.000000
O	1.917316	0.000000	0.000000
O	-1.917316	0.000000	0.000000
H	2.479474	0.000000	0.785072
H	2.479474	0.000000	-0.785072
H	-2.479474	0.785072	0.000000
H	-2.479474	-0.785072	0.000000

$\text{CuH}(\text{L-ascorbate})(\text{H}_2\text{O})_4^+$

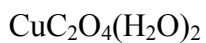
Element	X	Y	Z
Cu	-2.554119	0.204618	-0.182677
O	2.495659	-1.159318	2.512367
O	2.452051	-0.123655	0.482443
O	0.832979	2.264059	0.187868
O	2.921441	1.402529	-2.662114
O	-0.251520	-1.875139	2.006688
O	-0.902877	-0.653920	-0.701190
O	-1.802772	1.980765	0.480774
O	-2.984382	-1.344893	1.462135
O	-3.638265	-1.258716	-1.373516

O	-4.488981	1.096700	-0.188664
C	0.210170	-0.634730	-0.055714
C	0.533793	-1.180051	1.159370
C	1.917511	-0.858682	1.501999
C	1.476723	0.028661	-0.581649
C	1.324332	1.507831	-0.932285
C	2.611406	2.124521	-1.479680
H	0.282491	-2.124993	2.781107
H	1.856949	-0.495139	-1.462939
H	0.550722	1.582431	-1.699857
H	2.426476	3.184812	-1.685448
H	3.412119	2.041566	-0.733982
H	1.495728	2.278551	0.891165
H	3.769228	1.694906	-3.011156
H	-0.822376	2.131725	0.453305
H	-2.229187	2.799140	0.202579
H	-5.124762	0.619254	-0.737069
H	-4.976734	1.533791	0.518984
H	-2.135960	-1.697050	1.787704
H	-3.557018	-1.253973	2.232088
H	-3.692109	-2.023413	-0.782479
H	-3.169074	-1.562546	-2.161632

$\text{CuH(D-ascorbate)}(\text{H}_2\text{O})_4^+$

Element	X	Y	Z
Cu	1.338456	0.278439	2.323761
O	0.071296	1.001644	1.087992
O	3.072810	0.897735	1.231687
O	1.773378	-1.729001	1.305373
O	-0.285916	0.071930	3.660925
O	2.706954	0.025220	3.885105
O	1.836297	1.689085	-1.258622
O	0.437176	0.641637	-3.585234
O	-1.131435	-0.102936	-2.109935
O	-0.309048	-2.292050	-0.476613
O	-2.377214	-0.591814	1.927738
C	-0.098546	0.703108	-0.149174
C	0.661040	1.030157	-1.240427
C	0.029557	0.534435	-2.460046
C	-1.310506	-0.058681	-0.671084
C	-1.489555	-1.515966	-0.211950
C	-1.770799	-1.723141	1.289766
H	-2.225667	0.499580	-0.459825
H	-2.314597	-1.919188	-0.807171
H	-0.261507	-2.495742	-1.418672
H	-2.380007	-2.618680	1.425075
H	-0.818875	-1.901148	1.791013

H	-3.309482	-0.757823	2.100138
H	2.102750	1.825492	-2.183748
H	2.843084	1.455503	0.467547
H	3.464206	0.098983	0.853094
H	3.521725	0.542562	3.868942
H	2.519606	-0.218994	4.798761
H	-1.112200	0.003512	3.130698
H	-0.438922	0.769088	4.309435
H	1.151785	-2.028910	0.608694
H	2.088039	-2.518759	1.759410



Element	X	Y	Z
Cu	0.220299	0.001436	-0.001762
O	-1.136604	0.668638	1.127124
O	-1.137806	-0.672486	-1.125207
O	-3.370391	0.723223	1.234860
O	-3.371751	-0.739772	-1.222759
O	1.501827	0.874109	1.359112
O	1.503177	-0.864008	-1.365652
C	-2.354928	0.396973	0.678715
C	-2.355545	-0.407526	-0.671427
H	0.833390	1.221592	1.973878
H	2.155906	0.391795	1.877813
H	2.155176	-0.378487	-1.884016
H	0.837250	-1.215488	-1.980679

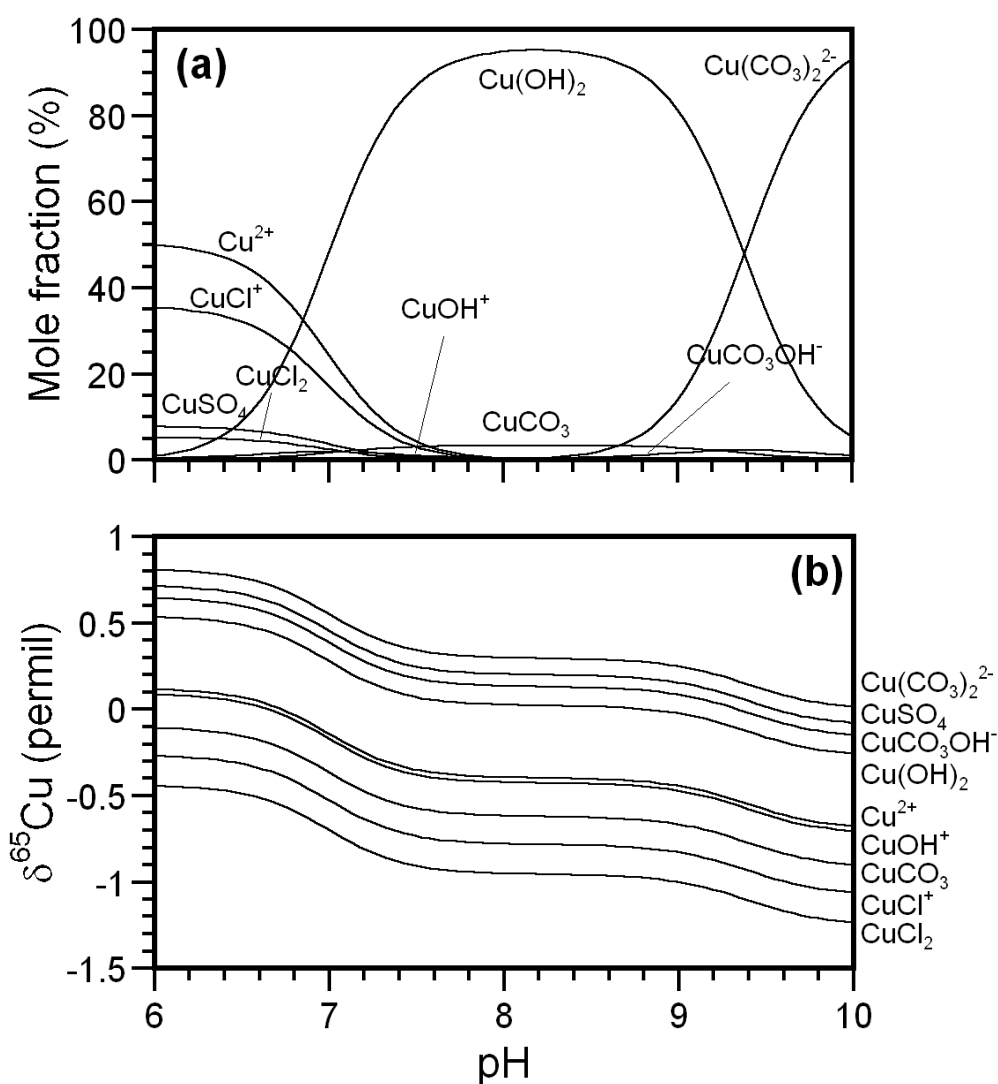


Figure S1. Mole fractions of Cu(II) species and Cu isotopic variations as functions of pH at 298 K. a) Mole fractions of Cu species, b) Species $\delta^{65}\text{Cu}$ relative to the bulk solution. Conditions are the same with those of Fig. 4 except for second hydrolysis constant. $\log^*\beta_2 = -16.65$ used in Fig. 4 was substituted by $\log \beta_2 = 14.3$ and ion product $\text{p}K_{\text{W}} = 14$ (ionic strength $I = 0$).